Published October 21, 2013

Golgi-associated RhoBTB3 targets Cyclin E for ubiquitylation and promotes cell cycle progression

Albert Lu and Suzanne R. Pfeffer

Department of Biochemistry, Stanford University School of Medicine, Stanford, CA 94305

Cyclin E regulates the cell cycle transition from G1 to S phase and is degraded before entry into G2 phase. Here we show that RhoBTB3, a Golgi-associated, Rho-related ATPase, regulates the S/G2 transition of the cell cycle by targeting Cyclin E for ubiquitylation. Depletion of RhoBTB3 arrested cells in S phase, triggered Golgi fragmentation, and elevated Cyclin E levels. On the Golgi, RhoBTB3 bound Cyclin E as part of a Cullin3 (CUL3)-dependent RING–E3 ubiquitin ligase complex comprised of RhoBTB3, CUL3, and RBX1. Golgi association of this complex was required for its ability to catalyze Cyclin E ubiquitylation and allow normal cell cycle progression. These experiments reveal a novel role for a Ras superfamily member in catalyzing Cyclin E turnover during S phase, as well as an unexpected, essential role for the Golgi as a ubiquitylation platform for cell cycle control.

Introduction

The S phase of the cell cycle represents a critical stage during which cells replicate their genetic material. E- and A-type cyclins together with their Cyclin-dependent kinase (CDK) partners play complementary roles in S-phase regulation (Woo and Poon, 2003). Cyclin E–CDK2 biological activity is associated with the onset and progression of S phase (Resnitzky et al., 1994; Ohtsubo et al., 1995). Cyclin E–CDK2 complexes phosphorylate multiple substrates that promote DNA replication and cell cycle progression (Errico et al., 2010). Monomeric (or "free") Cyclin E also performs cell cycle–related functions, independent of its association with CDK2 (Matsumoto and Maller, 2004; Geng et al., 2007).

The physiological relevance of Cyclin E is still under debate because mice lacking Cyclin E1 or E2 genes are viable and mice lacking both forms develop normally to embryonic day 10 (Geng et al., 2003). However, these mice show severe placental defects, suggesting that Cyclin E may be critical during endoreplicative cell cycles of trophoblast giant cells (Lee et al., 2009). It has been proposed that Cyclin A may be sufficient for DNA replication in cells continuously cycling, whereas Cyclin E may be required for cell cycle reentry from quiescence (Geng et al., 2003). Despite the controversy regarding the precise role of Cyclin E, it is clear that deregulation of Cyclin E levels can have catastrophic consequences for normal cell proliferation, as seen in a significant percentage of breast cancers, where high Cyclin E expression correlates with the stage and grade of the tumor (Enders, 2002; Hwang and Clurman, 2005; Potemski et al., 2006; Scaltriti et al., 2011). Thus, in mammals, Cyclin E expression and turnover are tightly regulated.

Our understanding of Cyclin E regulation remains incomplete. Cyclin E turnover is controlled by proteasomal degradation that is mediated by two independent, Cullin-RING ubiquitin ligase (CRL) pathways: the SCF (Skp1–CUL1–F-box protein) pathway that targets phosphorylated Cyclin E (Koepp et al., 2001), and a less-well characterized, Cullin 3 (CUL3) pathway that targets free, unphosphorylated Cyclin E (Singer et al., 1999).

Cullins are scaffolds for RING E3 ubiquitin ligase complexes (Petroski and Deshaies, 2005) that regulate a wide variety of cellular processes, including cell cycle progression, by targeting specific substrates such as Cyclins for ubiquitylation (Singer et al., 1999; Koepp et al., 2001; Santra et al., 2009). The basic molecular organization of CRLs consists of a Cullin family member that functions as a scaffold between a RING E3 ubiquitin ligase and one or more adaptor molecules that bind specific substrates. Thus, the adaptor molecules are responsible for dictating CRL substrate specificity. Each Cullin family member interacts with a specific class of adaptor molecules; CUL3–ubiquitin ligases employ BTB domain–containing proteins

Correspondence to Albert Lu: alulopez@stanford.edu; or Suzanne R. Pfeffer: pfeffer@stanford.edu

Abbreviations used in this paper: CRL, Cullin-RING ubiquitin ligase; CUL3, Cullin 3; SCF, Skp1–Cul1–F-box protein.

Supplemental Material can be found at:
http://jcb.rupress.org/content/suppl/2013/10/17/jcb.201305158.DC1.html

The Rockefeller University Press $30.00
J. Cell Biol. Vol. 203 No. 2 233–250
www.jcb.org/cgi/doi/10.1083/jcb.201305158

Published October 21, 2013

(BTB proteins) as substrate adaptors (Krek, 2003; Petroski and Deshaies, 2005). BTB proteins are characterized by their content of one or more BTB (Bric-a-brac, Tramtrack, Broad complex) domains that mediate protein–protein interactions (Perez-Torrado et al., 2006).

RhoBTB3 is a Golgi-localized BTB protein that is required for mannose 6-phosphate receptor transport from late endosomes to the TGN (Espinosa et al., 2009). RhoBTB3 belongs to a subfamily of atypical Rho GTPases that perform functions related to cell proliferation and membrane traffic by mechanisms that are still unclear (Siripurapu et al., 2005; Berthold et al., 2008b; Espinosa et al., 2009). The mammalian RhoBTB subfamily of proteins is comprised of three members, RhoBTB3 being the most divergent isoform (Berthold et al., 2008b). Unlike most Rho-related GTPases, RhoBTB3 binds and hydrolyzes ATP instead of GTP (Espinosa et al., 2009).

Here we show that Golgi-localized RhoBTB3 regulates Golgi membrane structure and S-phase cell cycle progression by a CUL3-dependent ubiquitylation pathway. RhoBTB3-depleted cells have a fragmented Golgi and are unable to divide. These cells are arrested in S phase and exhibit abnormally high levels of Cyclin E. RhoBTB3 interacts directly with Cyclin E and this interaction allows RhoBTB3 to present Cyclin E to a Golgi-localized CUL3–ubiquitin ligase complex into which RhoBTB3 assembles. Ultimately, RhoBTB3–CUL3 mediates ubiquitylation of this important cell cycle regulator both in vitro and in vivo, regulating its turnover during S phase—an essential event for normal cell cycle progression.

Results

RhoBTB3 regulates Golgi structure and cell size

We have shown previously that RhoBTB3 is required for mannose 6-phosphate receptor transport from late endosomes to the TGN (Espinosa et al., 2009). To understand further the role of RhoBTB3 in Golgi ribbon structure and function, we performed careful microscopic inspection of RhoBTB3-depleted cells. siRNA depletion of RhoBTB3 had a dramatic impact on Golgi morphology. Golgi complexes from HeLa cells treated for 72 h with two different RhoBTB3 siRNAs were consistently fragmented into smaller structures containing markers of both the trans (GCC185) and cis (GM130) Golgi (Fig. 1, A–D). Quantification revealed that 50–60% of RhoBTB3-depleted cells exhibited a fragmented Golgi, compared with ∼10% of control cells ($n \geq 400$ cells; Fig. 1 E).

The degree of Golgi fragmentation was slightly more prominent with siRNA #1 (Fig. 1, A–C), likely because of more efficient RhoBTB3 depletion (Fig. 1 D). Under these conditions, the microtubule cytoskeleton remained intact (Fig. 2 B), thus the phenotype observed was not due to microtubule disruption. In addition to Golgi fragmentation, the total cell size of RhoBTB3-depleted cells increased significantly, as judged by both light microscopy and flow cytometry analysis (Fig. 1, A and F; Fig. S1, A–C and E). The combined phenotype was also observed in another mammalian cell line, BsC-1 (not depicted). Finally, nuclei from RhoBTB3-depleted cells were approximately twofold larger and ∼25% of cells displayed micronuclei (Fig. S1, A, B, D, and E), a hallmark of genomic instability (Rajagopalan et al., 2004).

Control of S-phase progression by RhoBTB3

The phenotypical features observed suggested that depletion of RhoBTB3 resulted in a cell cycle–related dysfunction. Indeed, flow cytometry of cells treated either with or without siRNA indicated that RhoBTB3 plays a role in cell cycle control. Propidium iodide DNA staining followed by cell cycle analysis revealed an S-phase arrest (Fig. 2 A, bottom panels) after 48 and 72 h of RhoBTB3 depletion. In three different cell types, control siRNA-treated cells proliferated normally as revealed by microtubule staining of cells undergoing or finishing division; these cells displayed a typical mitotic spindle pattern (Fig. 2 B, top panel and inset). In contrast, RhoBTB3-depleted cells had a low mitotic index, consistent with their arrest in S phase (Fig. 2 B, bottom panel). Video microscopy further confirmed that RhoBTB3-depleted cells were unable to progress normally through the cell cycle and therefore did not reach mitosis, despite continuing to grow in size (Video 1).

Under normal physiological conditions, Cyclin E levels gradually increase throughout G1 and reach a peak at the G1/S transition. As cells progress through S phase, Cyclin E is ubiquitylated and degraded by the proteasome (Hwang and Clurman, 2005). Several groups have reported that deregulation of Cyclin E turnover results in impaired S-phase progression (Spruck et al., 1999; Willmarth et al., 2004; McEvoy et al., 2007). When we examined the level of Cyclin E after depletion of RhoBTB3, it was increased in two different cell types (Fig. 2, C and D; Fig. S2, A and B); under the same conditions, levels of S-phase Cyclin A2 or mitotic Cyclin B1 remained unchanged (Fig. 2 C).

High levels of Cyclin E correlate with elevated activity of its dependent kinase, CDK2 (Scaltriti et al., 2011). Accordingly, increased phosphorylation of a well-characterized Cyclin E–CDK2 substrate (Errico et al., 2010), retinoblastoma protein (p-RB), was detected in cells depleted of RhoBTB3 (Fig. 2 C). As reported previously under conditions of cyclin E overexpression (D'Assoro et al., 2002; Duensing, 2005; Koutsami et al., 2006), ∼10% of the cells showed centrosome overduplication, detected using anti-gamma tubulin antibodies, which was often accompanied by nuclear atypia and/or multiple nuclei (Fig. S2 C).

Cyclin–CDK complexes phosphorylate a wide range of cellular substrates including Golgi matrix proteins that are required for ribbon structure maintenance (Draviam et al., 2001; Errico et al., 2010; Pagliuca et al., 2011); these phosphorylation events have been shown to be responsible for triggering Golgi ribbon disassembly and fragmentation before mitosis (Colanzi et al., 2003). In this context, the Golgi fragmentation phenotype observed in RhoBTB3-depleted cells might be explained, in part, by an up-regulation of Cyclin E–CDK2 activities secondary to increased Cyclin E levels. Indeed, 75% of cells overexpressing exogenous Cyclin E–CDK2 displayed a fragmented Golgi (Fig. S3 A). However, loss of Cyclin E also a yielded a high percentage of cells containing a fragmented Golgi

Published October 21, 2013

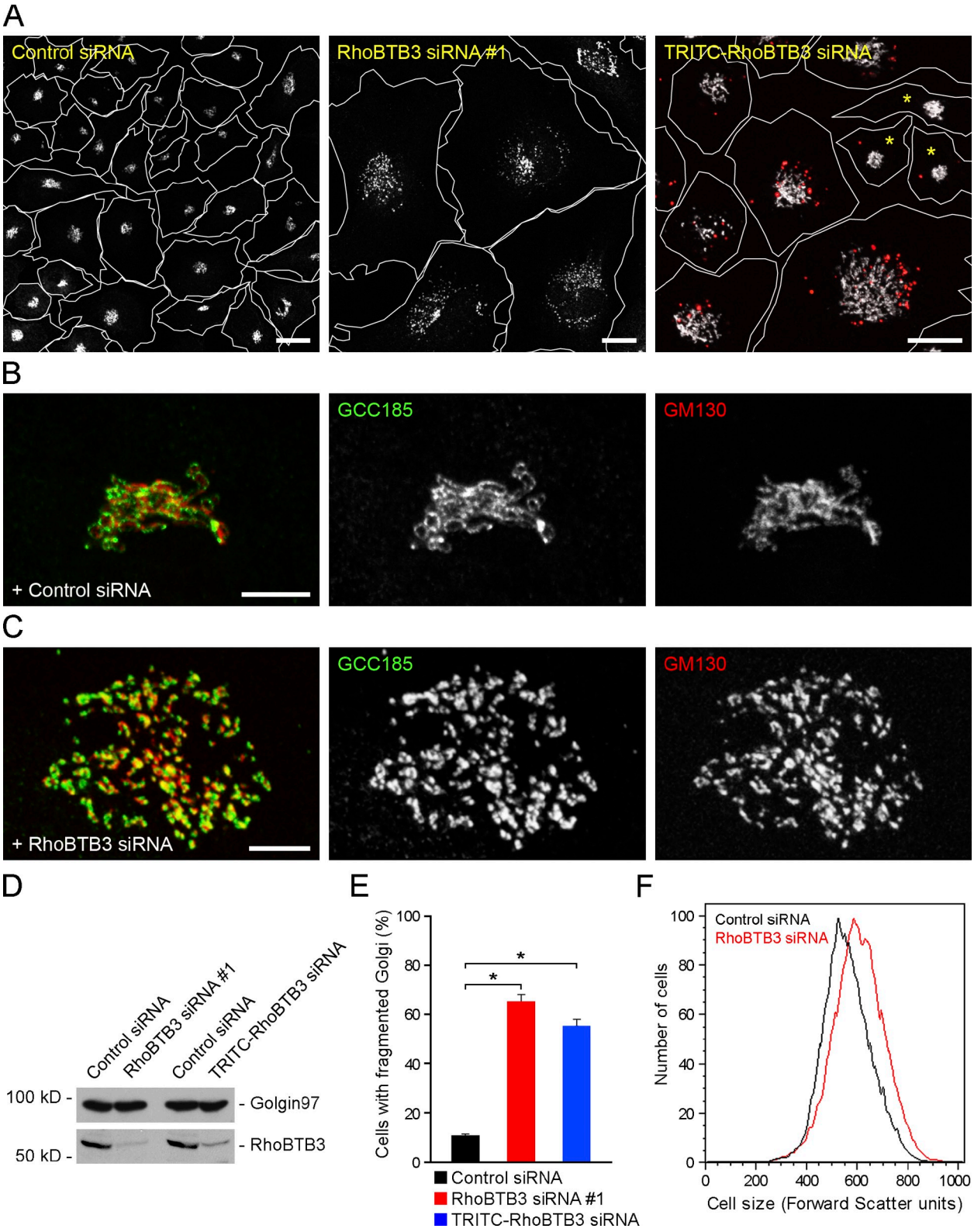

Figure 1. **RhoBTB3 depletion leads to Golgi fragmentation and increased cell size.** (A) Confocal microscopy of HeLa cells transfected for 72 h with control siRNA or two RhoBTB3 siRNAs as indicated and stained for GCC185. Red staining at right is TRITC-siRNA. Yellow asterisks indicate nondepleted cells. Bar, 20 µm. (B and C), High magnification of Golgi with control (B) or RhoBTB3-siRNA (C); anti-GCC185 is shown in green; anti-GM130 is shown in red. Merged images are presented in the far-left column. Bar, 8 µm. (D) Immunoblot detection of RhoBTB3 depletion in HeLa cells; molecular mass marker mobility is shown at the left in kilodaltons. (E) quantification of Golgi fragmentation in siRNA-treated cells. *t* test; *, $P < 0.05$; error bars represent SEM; $n = 3$. (F) flow cytometry analysis of cell size with the indicated siRNAs. A representative example from one of three independent experiments is shown.

Published October 21, 2013

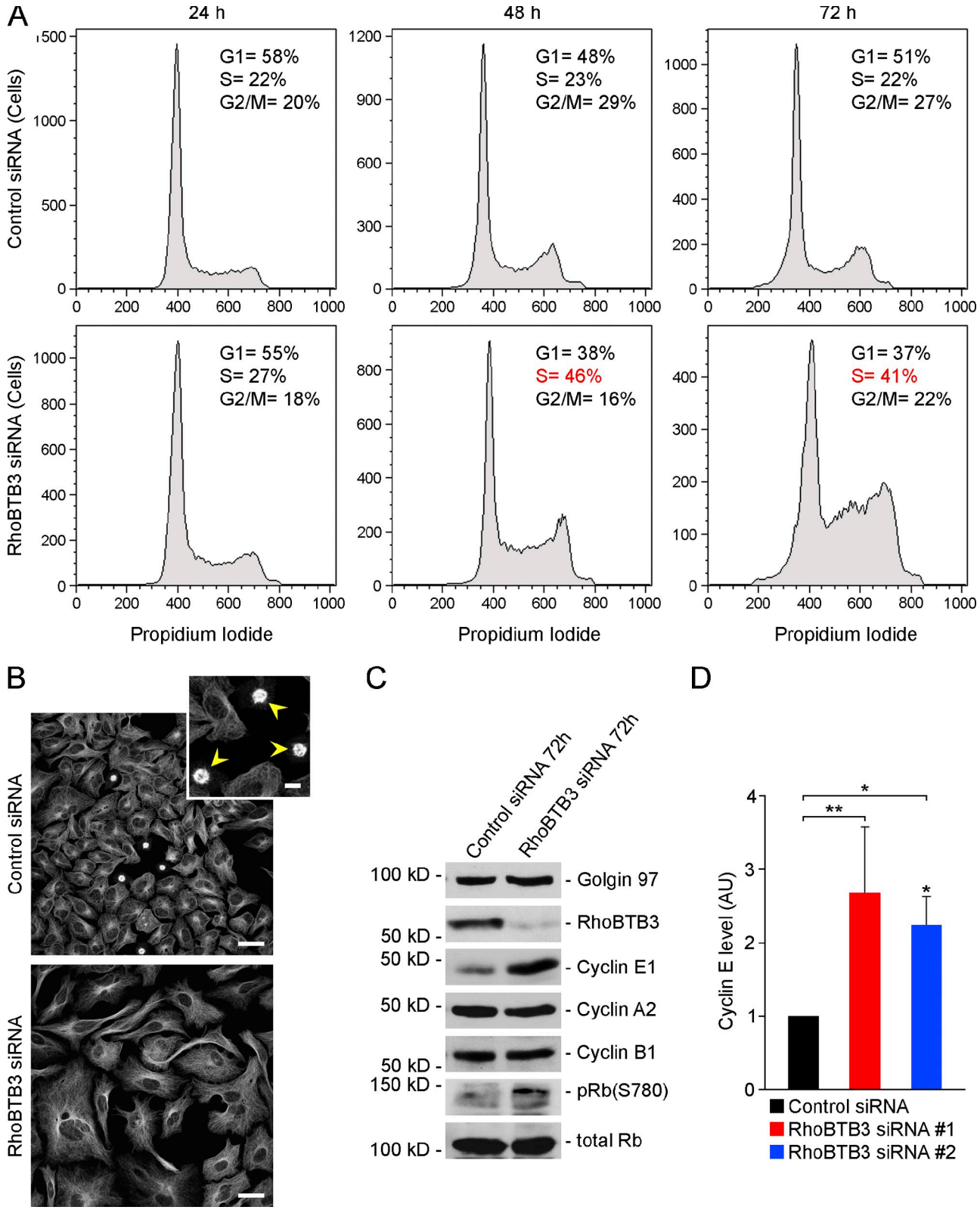

Figure 2. **S-phase arrest and Cyclin E stabilization in RhoBTB3-depleted cells.** (A) Flow cytometry of control or RhoBTB3-siRNA–treated cells at 24, 48, and 72 h after transfection. Propidium iodide staining was used to determine DNA content. A representative example from one of three independent experiments is shown. (B) Anti–α-tubulin staining of control and RhoBTB3-siRNA–treated cells. Arrowheads in inset indicate mitotic cells. Bar, 40 µm (inset, 10 µm). (C) Immunoblot detection of protein levels after 72 h with control or RhoBTB3-siRNA; molecular mass marker mobility is shown at left in kilodaltons. (D) Quantitation of protein levels from blots as in C. *t* test ;*, $P < 0.05$; **, $P < 0.01$; error bars represent SEM; $n \geq 3$.

Published October 21, 2013

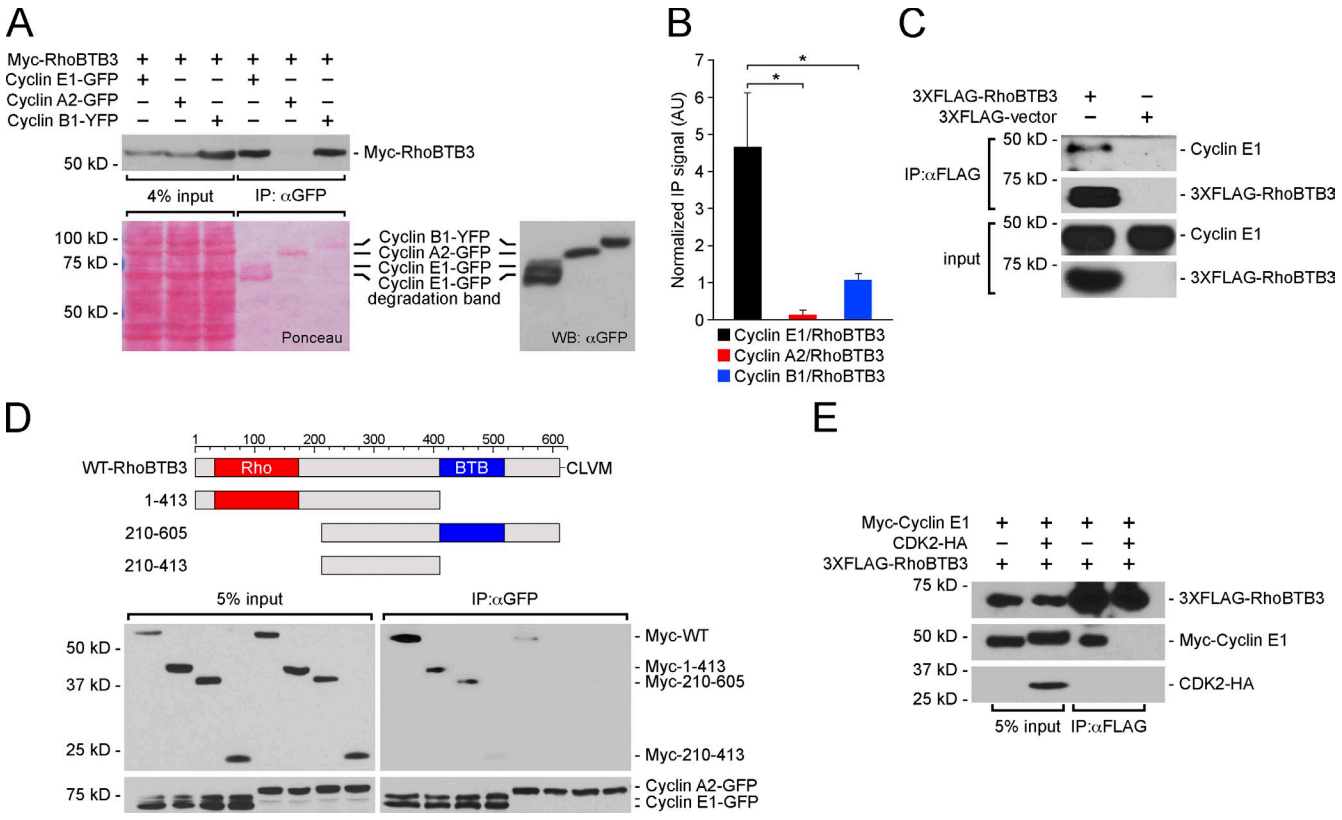

Figure 3. **RhoBTB3 interacts with free Cyclin E.** (A) HEK293T cells were transfected with the indicated constructs and immunoprecipitated with llama anti-GFP antibody. Samples were analyzed by immunoblot with mouse anti-Myc antibody (left portion) or rabbit anti-GFP (right portion). A Ponceau S–stained gel is shown at the bottom left. (B) Quantitation of RhoBTB3 in anti-Cyclin immunoprecipitates, normalized to inputs. *, $P < 0.05$; error bars represent SEM, $n \geq 3$. (C) Anti-FLAG immunoprecipitation of endogenous Cyclin E in cells transfected with FLAG-RhoBTB3. The input image was from a different exposure but confirms equal loading of the left and right lanes. (D) Schematic representation of RhoBTB3 and derived constructs. Bottom: cells were cotransfected with the indicated constructs and either Cyclin A2–GFP or Cyclin E1–GFP; immunoprecipitation was performed as in A. (E) Cells cotransfected with FLAG-RhoBTB3, Myc–Cyclin E1, or CDK2-HA were analyzed by immunoprecipitation and blotting as in C. Molecular mass marker mobility is shown at the left in kilodaltons.

(Fig. S3, B, D, and E), but their overall cell size remained similar to that of control cells (Fig. S3 B). Finally, the combination of Cyclin E and RhoBTB3 siRNAs resulted in Golgi fragmentation and increased cell size (Fig. S3, C–E). Altogether, these results suggest a complex role for Cyclin E in Golgi structure regulation. In addition, high overexpression of RhoBTB3 dramatically altered Golgi morphology (Fig. S3 F, red asterisks), consistent with a dominant role for this protein.

Cyclin E interacts with RhoBTB3 as a putative substrate

RhoBTB3 has been shown to interact with CUL3 via its BTB domain (Berthold et al., 2008a). For this reason, we tested the possibility that RhoBTB3, in its role as a CUL3 substrate adaptor, binds Cyclin E. As shown in Fig. 3, RhoBTB3 coimmunoprecipitated with Cyclin E1-GFP but not Cyclin A2-GFP, another S-phase Cyclin (Fig. 3, A and B). RhoBTB3 also bound Cyclin B1 (Fig. 3 A), but to a lesser extent than Cyclin E1 (Fig. 3, A and B). The relevance of the interaction between RhoBTB3 and Cyclin E was further confirmed by immunoprecipitating endogenous Cyclin E with a FLAG-tagged RhoBTB3 (Fig. 3 C). Because our data pointed to a role for RhoBTB3 during S phase, we focused on S-phase Cyclins. To further characterize the RhoBTB3–Cyclin E interaction, we tested the ability of different RhoBTB3 truncation constructs to bind Cyclin E1 (Fig. 3 D). Constructs comprised of RhoBTB3 residues 1–413 or residues 210–605 bound Cyclin E1, albeit to a lesser extent compared with the full-length protein; in contrast, a peptide representing residues 210–413 failed to bind (Fig. 3 D). These data suggest that both N-terminal and C-terminal residues in RhoBTB3 coordinate binding to Cyclin E, either directly or by creating a stably folded binding domain. Finally, expression of CDK2 abolished the interaction of RhoBTB3 with Cyclin E (Fig. 3 E), indicating that RhoBTB3 interacts with free Cyclin E.

RhoBTB3 is a molecular component of a Golgi-localized CUL3-ubiquitin ligase

RhoBTB3 resides on the Golgi (Espinosa et al., 2009). Therefore, if RhoBTB3 directs Cyclin E into a CUL3-mediated ubiquitylation pathway, CUL3 should colocalize and interact with RhoBTB3 on the Golgi. Indeed, in both HeLa (Fig. 4 A) and HEK293T (not depicted) cells a pool of CUL3 was detected on the Golgi, as previously shown (Singer et al., 1999), where it colocalizes with RhoBTB3 and GCC185 (Fig. 4 A). We also confirmed that RhoBTB3 interacts with CUL3 (Fig. 4, B and C; Berthold et al., 2008a; Bennett et al., 2010).

Published October 21, 2013

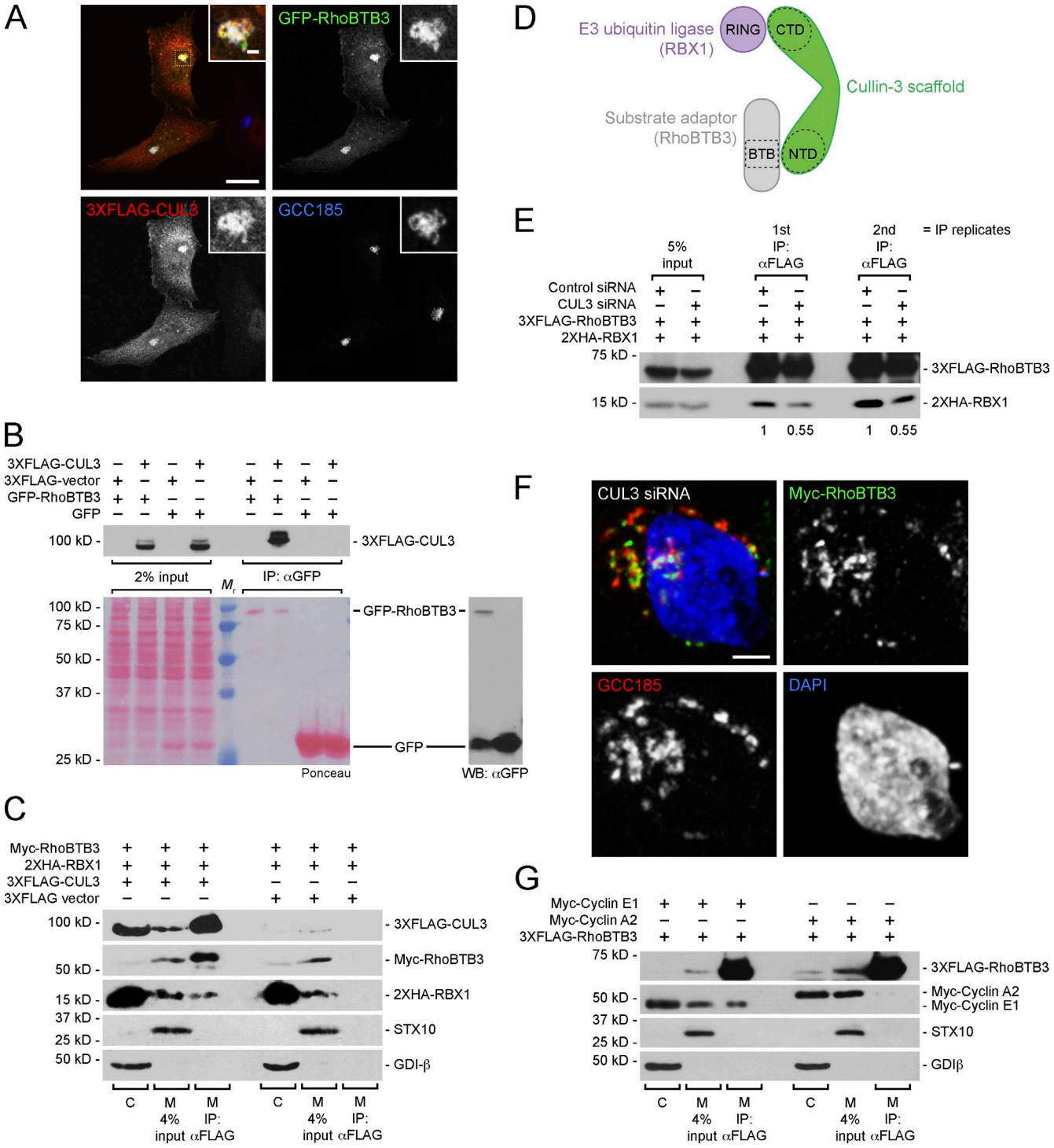

Figure 4. **RhoBTB3 is part of a CUL3–ubiquitin ligase complex on the Golgi that targets Cyclin E.** (A) Colocalization of transfected GFP-RhoBTB3 and FLAG-CUL3 on the Golgi of HeLa cells, detected with anti-GCC185 antibodies. Bar, 20 µm. Insets, enlarged Golgi regions. Bar, 2 µm. (B) GFP-RhoBTB3 binds 3XFLAG-CUL3. Total cell extract inputs (2%) are shown at left; anti-GFP bound material is shown at right, detected by immunoblot. (C) Interaction of RhoBTB3 with FLAG-CUL3 and HA-RBX1 in membranes from HEK293T cells. Cells were transfected as indicated at the top, immunoprecipitated with anti-FLAG antibody, and bound proteins detected by immunoblot with antibodies to the proteins indicated at right. Molecular mass marker mobility is shown at the left in kilodaltons. C, cytosol; M, membrane. (D) Schematic diagram of a canonical CUL3–ubiquitin ligase complex. The N-terminal domain (NTD) of CUL3 interacts with the RING E3 ubiquitin ligase RBX1; the C-terminal domain (CTD) binds a BTB domain–containing substrate adaptor (i.e., RhoBTB3). (E) Interaction of FLAG-RhoBTB3 with HA-RBX1 after 72 h of control or CUL3 siRNA depletion in HEK293T cells. Inputs are at left (5%); anti-FLAG precipitates in duplicate are at right, immunoblotted with anti-FLAG (top) or anti-HA (bottom). Quantitation of coprecipitated RBX1 is shown in relative values at the bottom of the anti-HA panel. (E) CUL3 depletion disrupts the Golgi but does not release RhoBTB3 from the Golgi. Bar, 5 µm. (F) Interaction of RhoBTB3 with Cyclin E on membranes. Membrane extracts from cells cotransfected with indicated constructs were immunoprecipitated and analyzed as in C. Molecular mass marker mobility is shown at the left in kilodaltons.

Published October 21, 2013

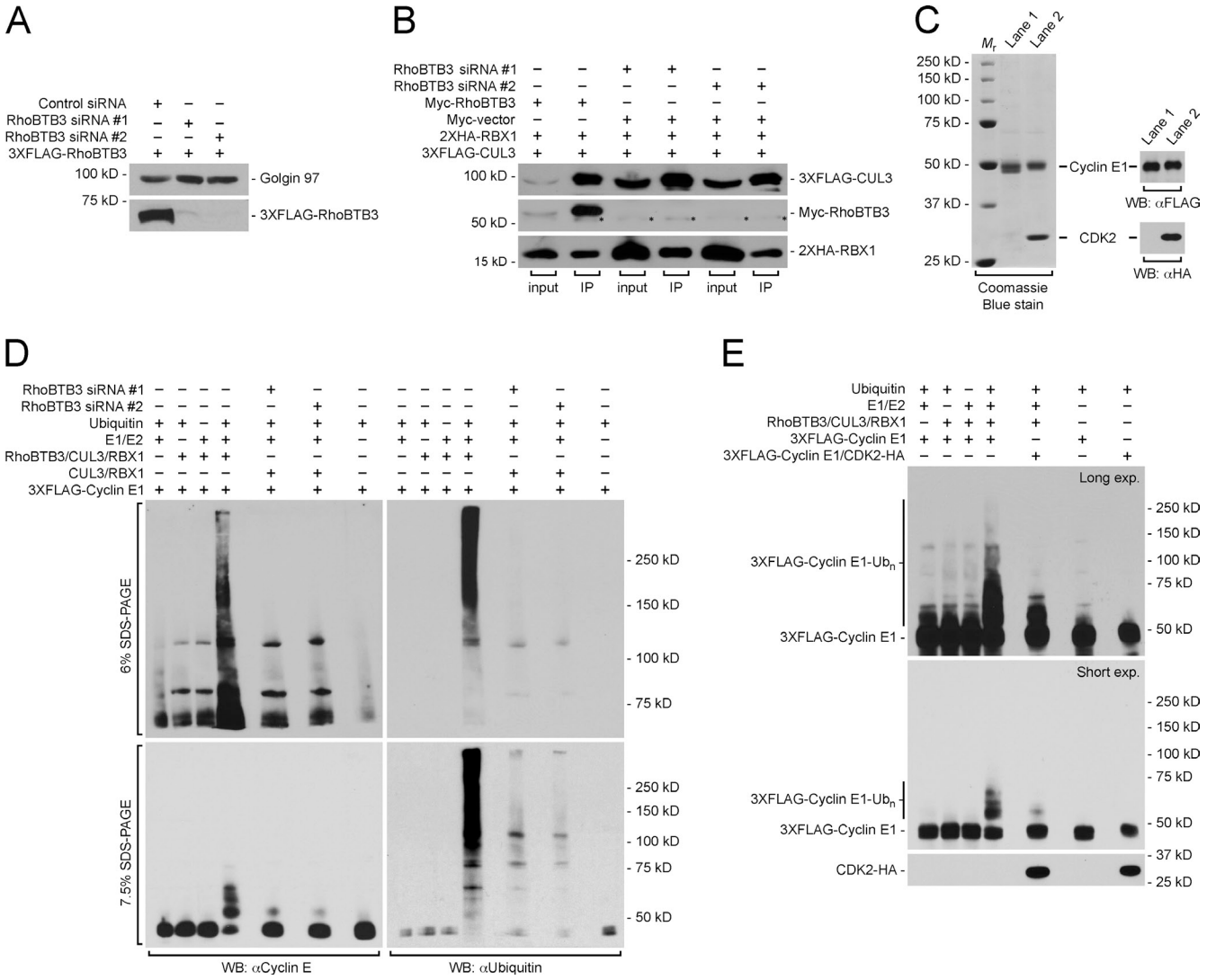

Figure 5. **In vitro reconstitution of Cyclin E ubiquitylation by a RhoBTB3$^{CUL3/RBX1}$ ubiquitin ligase complex.** (A) RhoBTB3 depletion in HEK293T cells assayed by immunoblot; Golgin 97 was used as a loading control. (B) Characterization of anti-FLAG immunopurified complexes containing Myc-RhoBTB3, FLAG-CUL3, and HA-RBX1 proteins; asterisks indicate a nonspecific band. (C) Coomassie blue gel and immunoblot analysis of purified FLAG–Cyclin E1 (lane 1) and FLAG–CyclinE1–CDK2-HA complex (lane 2) isolated by immunoprecipitation from HEK293T cells. (D) In vitro–reconstituted ubiquitylation of Cyclin E using complexes shown in B. Left columns, anti–Cyclin E immunoblots; right columns, anti-ubiquitin immunoblots. Top gel, 6% to show larger species; bottom gel, 7.5% to include Cyclin E. Quantitation of lanes 1–7 of the bottom gels gave relative values of: 0.05, 0.06, 0.05, 1, 0.16, 0.09, and 0.06 (left); 0, 0, 0, 1, 0.1, 0.05, and 0 (right). (E) In vitro ubiquitylation of Cyclin E or Cyclin E–CDK2 complex as in D; top panel represents a long exposure of the same gel shown below (blotted using anti–Cyclin E). At the bottom is shown a blot for CDK2-HA in the same samples. Quantitation of lanes 1–7 gave relative values of: 0.3, 0.3, 0.3, 1, 0.4, 0.1, and 0 (long exposure). Molecular mass marker mobility is shown at the left (A–C) or right (D and E) in kilodaltons.

CUL3–ubiquitin ligases consist of a CUL3 scaffold that bridges a BTB protein and a RING domain E3 ubiquitin ligase (i.e., RBX1; Fig. 4 D). The N terminus of CUL3 interacts with the BTB domain of BTB proteins, while the C terminus binds RBX1 (Zheng et al., 2002; Furukawa et al., 2003; Pintard et al., 2003; Xu et al., 2003). Consistent with the presence of RhoBTB3 in a CUL3–RING E3 ligase complex on membranes where RhoBTB3 resides, immunoprecipitation of CUL3 from membranes coprecipitated RhoBTB3 and the RING E3 ubiquitin ligase, RBX1, suggesting that they may be part of a ternary complex (Fig. 4 B). In agreement with this, CUL3 depletion followed by immunoprecipitation of RhoBTB3 showed around 50% reduction of coprecipitated RBX1 compared with Control siRNA-treated cells (Fig. 4 E).

It has been suggested that complex formation is required for proper targeting of either CUL3 or its BTB protein partner to specific subcellular locations because depletion of either molecule results in mislocalization of its counterpart (Maerki et al., 2009). This might not be the case for the RhoBTB3$^{CUL3/RBX1}$ complex, however, because depletion of CUL3 did not influence the Golgi localization of RhoBTB3 (Fig. 4 F). CUL3-depleted cells also displayed significant Golgi fragmentation (Fig. S4, A–C), a finding that supports the idea that ubiquitylation events influence Golgi structure (Litterman et al., 2011; Tang et al., 2011). In addition, as previously reported (McEvoy et al., 2007; Maerki et al., 2009), loss of CUL3 led to increased cell size and an increase in the number of multinucleated cells (Fig. S4 D).

Published October 21, 2013

Finally, we predicted that RhoBTB3 interaction with Cyclin E should be achieved on membranes. Both endogenous and transfected Cyclin E could be detected in nuclear, cytosolic, and membrane fractions of two different cell types, although their relative amounts in each of these compartments varied significantly (Fig. S5, A–F). Nevertheless, membrane associated Cyclin E was detected in both HeLa and HEK293T cells, before and after transfection with recombinant Cyclin E1 (Fig. S5, A–F). Binding of FLAG-RhoBTB3 to Cyclin E but not to Cyclin A was detected upon immunoprecipitation of membrane fractions (Fig. 4 G). This interaction provides a possible explanation for why Cyclin E can be detected in Golgi fractions (Gaulin et al., 2000). Collectively, these data suggest that RhoBTB3 targets Cyclin E to a Golgi-localized CUL3 ubiquitylation pathway.

Regulation of Cyclin E ubiquitylation and stability by RhoBTB3$^{CUL3/RBX1}$ during S phase

To demonstrate that RhoBTB3$^{CUL3/RBX1}$ mediates Cyclin E ubiquitylation, we reconstituted this process in vitro. FLAG-tag affinity chromatography was used to immunopurify RhoBTB3$^{CUL3/RBX1}$ complexes from cells transfected with FLAG-CUL3 together with Myc-RhoBTB3 and HA-tagged RBX1. Although addition of "complete" complexes yielded efficient ubiquitylation of purified Cyclin E (Fig. 5 D), reactions containing a RhoBTB3-deficient complex obtained from cells treated with two different RhoBTB3 siRNAs (Fig. 5, A and B) showed a significant reduction in Cyclin E ubiquitylation (Fig. 5 D), highlighting a direct role for RhoBTB3 in this process (note that the left panels in Fig. 5 D show immunoprecipitated Cyclin E ubiquitylation; the right panels show total ubiquitylation and may include ubiquitylated RhoBTB3 protein. The top gel is a dark exposure of a 6% gel to highlight polyubiquitinated species; the bottom gel is higher percentage and lower exposure to include unmodified Cyclin E). Consistent with the finding that RhoBTB3 interacts with free Cyclin E1 (Fig. 3 E), purified Cyclin E1 in complex with CDK2 failed to be ubiquitylated, compared with monomeric Cyclin E1 (Fig. 5, C and E), indicating that RhoBTB3$^{CUL3/RBX1}$ targets uncomplexed Cyclin E1.

To rule out any possible cross-contamination of immunopurified RhoBTB3 complexes, we reconstituted the complex using only bacterially expressed components. Specifically, RhoBTB3$^{CUL3/RBX1}$ ubiquitin ligase was assembled in vitro by mixing coexpressed GST-CUL3 and HA-RBX1 with purified FLAG-RhoBTB3 protein (Fig. 6 A). This complex was then used to ubiquitylate bacterially expressed GST-Cyclin E (Fig. 6 B). As shown in Fig. 6 C, we observed a time-dependent increase in ubiquitylation of nonphosphorylated, "free" GST-Cyclin E1 in the presence of complex containing RhoBTB3. After 60 min, the level of Cyclin E1 ubiquitylation by recombinant RhoBTB3$^{CUL3/RBX1}$ was similar to that obtained using the immunopurified complex obtained from mammalian cells (Fig. 5 B and Fig. 6 C, far right lane).

To confirm these results in vivo, we depleted RhoBTB3 protein from cells and analyzed the ubiquitylation status of Cyclin E. RhoBTB3 siRNA-treated cells showed a substantial decrease in Cyclin E ubiquitylation compared with control siRNA-treated cells (Fig. 7 A). Consistent with this finding, overexpression of RhoBTB3 led to increased Cyclin E ubiquitylation (Fig. 7 B). Thus, in vivo, RhoBTB3 regulates Cyclin E ubiquitylation.

Cyclin E protein stability is regulated by ubiquitylation followed by proteasomal degradation (Hwang and Clurman, 2005). Our data suggested that depletion of RhoBTB3 should result in increased Cyclin E stability. To test this, Cyclin E levels were determined at different time points after addition of the protein synthesis inhibitor cycloheximide, in control or RhoBTB3 siRNA-treated cells (Fig. 7 C). In the absence of RhoBTB3, Cyclin E was significantly more stable when compared with control conditions over a 5-h period (Fig. 7 C, graph). Cyclin E levels decreased ∼40% in control siRNA-depleted cells after 1 h; in contrast, in RhoBTB3-depleted cells, Cyclin E remained high over 3 h.

If RhoBTB3 controls Cyclin E levels, it may also be upregulated during S phase. Indeed, RhoBTB3 protein levels increased during S phase after Cyclin E levels plateaued; RhoBTB3 peaked while Cyclin E levels dropped significantly (Fig. 7 D). Altogether, these results highlight a tight connection between RhoBTB3 and Cyclin E and show that a RhoBTB3$^{CUL3/RBX1}$-mediated ubiquitylation pathway regulates Cyclin E turnover.

Golgi localization is required for proper RhoBTB3 function

The observation that CUL3 depletion does not lead to RhoBTB3 mislocalization (Fig. 4 F), together with the finding that exogenous CUL3 was detected on the Golgi only when cotransfected with RhoBTB3 (unpublished data) support the proposal that RhoBTB3 contributes to the association of RhoBTB3$^{CUL3/RBX1}$ complexes with Golgi membranes, although other Golgi-associated BTB proteins (Nacak et al., 2006) may also contribute to the recruitment of CUL3 to this compartment.

How does RhoBTB3 associate with the Golgi to mediate Cyclin E ubiquitylation? The intracellular localization of different Myc-tagged versions of RhoBTB3 was analyzed by microscopy to address this question (Fig. 8 A). Full-length, Myc-tagged RhoBTB3 localized to the Golgi (Fig. 8 B), as did GFP-RhoBTB3 (Fig. 4 A). Analysis of a variety of truncation constructs is summarized in Fig. 8. Loss of residues 415–607 abolished Golgi localization, yet this domain alone was not sufficient for localization. Residues 1–210, on the other hand, were dispensable for Golgi localization: a construct comprised of RhoBTB3 residues 210–605 (Fig. 8 H) showed proper Golgi targeting. This is a rather large targeting domain and suggests that a specific, three-dimensional surface is needed for proper Golgi association. Golgi recruitment did not require RhoBTB3's C-terminal CAAX motif (Fig. 8 C), which is a site for prenylation in other GTPases and often directs membrane targeting (Zhang and Casey, 1996). Release of RhoBTB3 from membranes incubated with either high salt or basic pH buffer (Fig. 8 L) confirmed that RhoBTB3 is peripherally associated with the Golgi membrane surface and most (but not all) of it is membrane associated at steady state (Fig. 8 L).

To test if Golgi localization was required for RhoBTB3-mediated cell cycle control, we performed rescue experiments

Published October 21, 2013

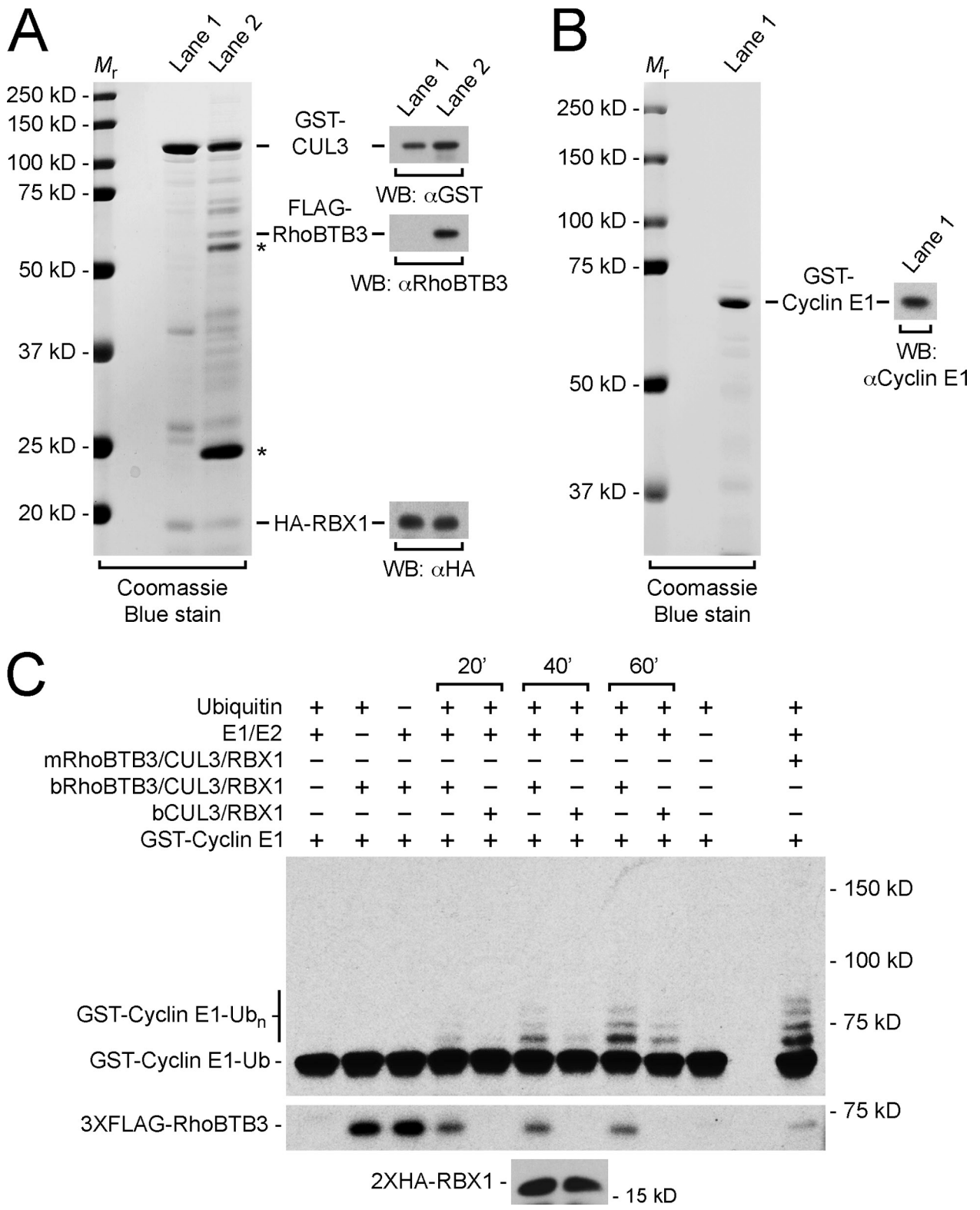

Figure 6. **Unphosphorylated Cyclin E is a substrate of recombinant RhoBTB3$^{CUL3/RBX1}$ in vitro.** (A) CUL3–RBX1 binary complexes (lane 1 in Coomassie blue gel and immunoblot) were purified from *E. coli* coexpressing both GST-CUL3 and HA-RBX1. Assembly of RhoBTB3$^{CUL3/RBX1}$ complex was performed by mixing CUL3–RBX1 with purified FLAG-RhoBTB3 bound to anti-FLAG antibody–conjugated agarose. Coomassie blue staining and immunoblot analysis of ternary complexes eluted with 0.2 mg/ml FLAG peptide are shown in lane 2 of gel and blot. Asterisks indicate IgG heavy and light chains. (B) Coomassie blue staining and immunoblot analysis of GST–Cyclin E1 purified with glutathione-Sepharose from *E. coli* (lane 1 in gel and blot). (C) Time course of RhoBTB3$^{CUL3/RBX1}$ -dependent ubiquitylation of GST–Cyclin E1 using recombinant complexes shown in A; mRhoBTB3–CUL3–RBX1 or bRhoBTB3–CUL3–RBX1 complexes were purified from mammalian cells or bacteria, respectively; bCUL3–RBX1 binary complex was purified from bacteria. The presence of RhoBTB3 in each reaction (middle blot) was detected using anti-RhoBTB3 antibody. As a control, bottom blot shows similar levels of RBX1 present in the 40-min reactions. Molecular mass marker mobility is shown at left (A and B) or right (C) in kilodaltons.

Published October 21, 2013

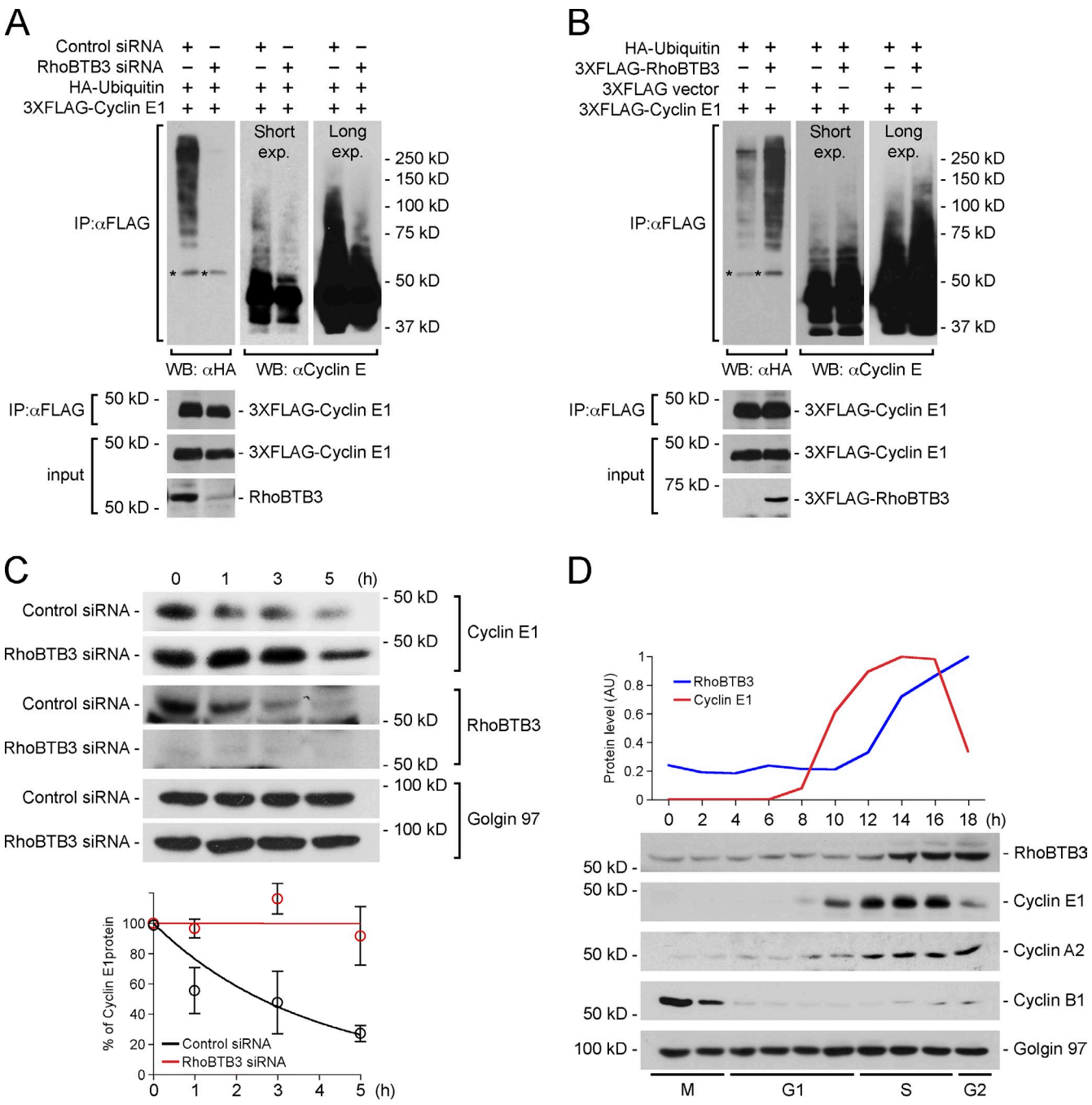

Figure 7. **RhoBTB3-mediated regulation of Cyclin E ubiquitylation and stability in vivo.** (A) Immunoblot detection of Cyclin E1 ubiquitylation in HeLa cells treated with control or RhoBTB3-siRNA #1. After 48 h, cells were transfected with FLAG–CyclinE1 and HA-ubiquitin; after 72 h total, extracts were precipitated with anti-FLAG antibody, eluted with 0.2 mg/ml FLAG peptide, and blotted using anti-HA (left panel) or anti–Cyclin E (right panels). The far right panel is a longer exposure (Long exp.) of the middle panel (Short exp.). Bottom, immunoprecipitated FLAG–Cyclin E1 and input (5%). (B) Exogenous RhoBTB3 expression increases Cyclin E1 ubiquitylation. Analysis was as in A; RhoBTB3 was transfected in HeLa cells 12 h before other components, and samples were collected 24 h later. Asterisks indicate IgG heavy chain. (C) Determination of Cyclin E stability. U2OS cells transfected for 72 h with either control or RhoBTB3 siRNA were treated with 50 µg/ml cycloheximide as indicated and Cyclin E levels determined by immunoblotting. Graph shows mean Cyclin E level for each time point (circles) from at least two independent experiments; error bars represent SEM. (D) Synchronized HeLa cells (Hengst et al., 1994) were analyzed for their content of the proteins indicated at right, monitored by immunoblot at the indicated times after release of thymidine-nocodazole block. A representative example from one of two independent experiments is shown. Graph represents quantitation of the blots below. Molecular mass marker mobility is shown at the right (A and B) or left (D) in kilodaltons.

using either an siRNA-resistant, wild-type RhoBTB3 construct that localizes to the Golgi or a minimally truncated version, comprising residues 1–525 that does not associate with the Golgi but retains both its Rho-like and BTB domains (Fig. 8, A and E). It is well established that Cyclin E begins to accumulate in the nucleus during the G1-to-S phase transition (Ekholm et al., 2001; Sütterlin et al., 2002). Thus, the percentage of nuclear Cyclin E–positive cells correlates with the proportion of cells in late G1 and S phase (Dulić et al., 1992; Koff et al., 1992; Ekholm et al., 2001), which would be predicted to increase

Published October 21, 2013

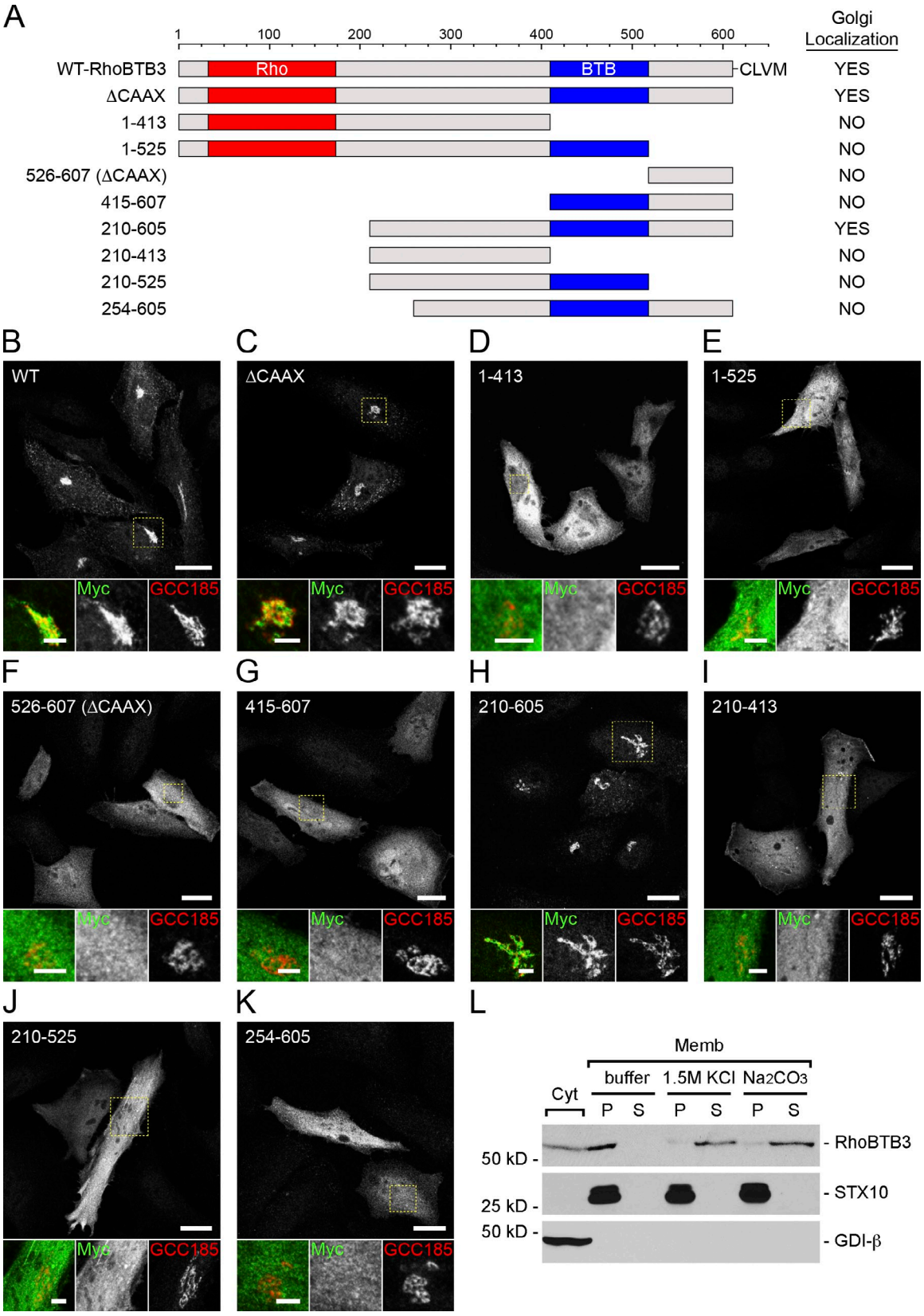

Figure 8. **Determinants of RhoBTB3 targeting to the Golgi.** (A) Diagram of N-terminally Myc-tagged constructs; the Rho domain is shown in red and the BTB domain in blue. (B–K) Immunofluorescence microscopy of the localization of the indicated constructs in HeLa cells, detected with anti-Myc antibody. Bar, 20 µm. Insets show enlarged Golgi regions, identified using anti-GCC185 antibody. Bars (insets), 5 µm. (L) RhoBTB3 is a peripheral membrane protein. After 10 min on ice with the treatments indicated, membrane-associated or soluble fractions were obtained by centrifugation at 100,000 *g* and analyzed by immunoblot. Syntaxin 10 was used as an internal membrane control; GDI-β served as a cytosolic marker protein. Molecular mass marker mobility is shown at the left in kilodaltons.

Published October 21, 2013

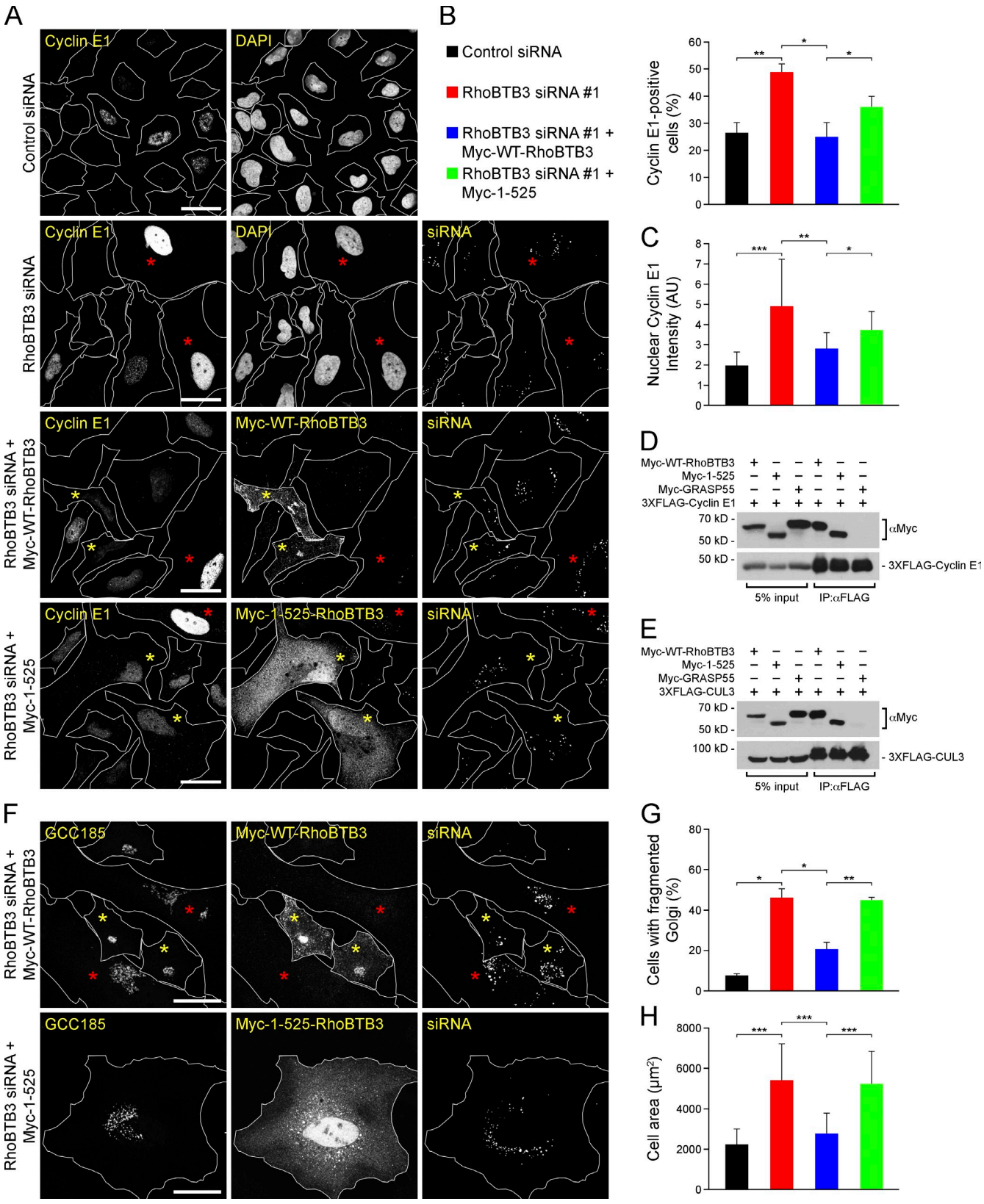

Figure 9. **Golgi localization is required for RhoBTB3 regulation of Cyclin E levels, Golgi structure, and cell size.** (A) HeLa cells were treated with Control (top) or RhoBTB3 siRNA (as indicated) for 72 h. After 24 h, cells were transfected with plasmid encoding siRNA-resistant Myc-tagged WT-RhoBTB3 or Myc-tagged 1–525 truncation. Left column, Cyclin E1 detected with mouse anti–Cyclin E (HE12). Middle (in top and second panels), nuclei stained with DAPI; right column, TRITC-labeled RhoBTB3 siRNA #1. Red asterisks indicate siRNA-transfected cells, yellow asterisks indicate cells transfected with siRNA and rescue plasmid. Bars, 40 µm. (B and C) Quantification of rescue. Control siRNA (black column), RhoBTB3 siRNA (red column), RhoBTB3 siRNA + WT rescue construct (blue column), and RhoBTB3 siRNA + 1–525 rescue construct (green column). The percentages of Cyclin E–positive cells (B) and nuclear

Published October 21, 2013

during an S-phase arrest due to deregulation of Cyclin E turnover (Spruck et al., 1999; Willmarth et al., 2004; McEvoy et al., 2007).

Consistent with our earlier findings, RhoBTB3 depletion resulted in a 1.6-fold increase in the proportion of Cyclin E1–positive cells (Fig. 9, A and B). Under these conditions, the cell-associated, integrated intensity of nuclear Cyclin E staining also increased significantly (Fig. 9 C). Expression of wild-type RhoBTB3 in depleted cells not only restored the percentage of Cyclin E–positive cells to values similar to those seen in control siRNA-treated cells (Fig. 9, A and B), but it also decreased the nuclear Cyclin E integrated intensity by 50% (Fig. 9 C). In contrast, Golgi-mislocalized truncated RhoBTB3 was less potent in reducing both the proportion of Cyclin E–positive cells and the nuclear Cyclin E level per cell (Fig. 9, A–C). Importantly, despite these differences, both RhoBTB3 constructs were able to bind the putative substrate (Cyclin E) and the ubiquitin ligase scaffold (CUL3), whereas the unrelated peripheral Golgi protein GRASP55 did not (Fig. 9, D and E). Finally, the Golgi fragmentation phenotype and increased cell size of RhoBTB3-depleted cells were also rescued by the wild-type but not by the Golgi-mislocalized version of the protein (Fig. 9, F–H). Altogether, these data demonstrate that Golgi localization is critical for RhoBTB3's role in Golgi homeostasis and S-phase cell cycle control, beyond Cyclin E and CUL3 interaction.

RhoBTB3$^{CUL3/RBX1}$ as an alternative pathway in Cyclin E ubiquitylation

In mammalian cells, the SCF-FBW7 pathway also plays a major role in ubiquitylation-dependent regulation of Cyclin E (Koepp et al., 2001; Hwang and Clurman, 2005; Welcker and Clurman, 2008). In an effort to demonstrate that RhoBTB3 represents an alternative ubiquitylation pathway, HEK293T cells were treated with an siRNA targeting all isoforms of Fbw7 (Fig. 10 A), the Cyclin E substrate adaptor for the SCF ubiquitin ligase (Hao et al., 2007). As previously reported (Koepp et al., 2001), Fbw7 depletion resulted in increased Cyclin E levels (Fig. 10 A). Immunopurified RhoBTB3$^{CUL3/RBX1}$ complexes from both control or Fbw7 siRNA-depleted cells (Fig. 10 B) catalyzed ubiquitylation of Cyclin E in vitro with similar efficiencies (Fig. 10 C), confirming that our previous in vitro data were not influenced by the presence of co-immunopurified SCF-FBW7 ubiquitin ligase (Fig. 7, D and E). On the other hand, in vivo overexpression of RhoBTB3 resulted in around 50% reduction of the increased Cyclin E levels observed under Fbw7 depletion conditions (Fig. 10 D). These results confirm our contention that Golgi-associated RhoBTB3$^{CUL3/RBX1}$ represents an alternative pathway that mediates Cyclin E ubiquitylation in human cells (Fig. 10, E and F).

Discussion

We have shown here that Golgi-associated RhoBTB3 appears to promote cell cycle progression by functioning as an adaptor protein that can present Cyclin E to the CUL3 ubiquitination machinery. In the absence of RhoBTB3, cells arrest in S phase and display a fragmented Golgi apparatus, concomitant with an increase in Cyclin E levels (Fig. 10 F). RhoBTB3 was previously shown to be a Rab9 GTPase effector that is required for the transport of proteins from late endosomes to the Golgi complex (Espinosa et al., 2009). The fact that RhoBTB3, an atypical Rho family member, can influence cell cycle progression by ubiquitylation reveals an unexpected role for a Golgi protein that functions in membrane traffic (Espinosa et al., 2009) and regulates Golgi compartment integrity from its central location at the Golgi.

The Golgi apparatus plays critical regulatory roles at multiple stages of the cell cycle. Cells require fragmentation of the Golgi complex to be able to enter mitosis (Sütterlin et al., 2002). This so-called "Golgi checkpoint" involves Cyclin B–CDK1 phosphorylation of Golgi matrix proteins and subsequent recruitment of polo-like kinase (Preisinger et al., 2005) and Aurora kinase to the centrosome (Persico et al., 2010). In this manner, the Golgi and centrosome are two closely associated organelles that communicate with each other during the cell cycle. It is interesting to note that entry into S phase and initiation of DNA replication requires centrosomal localization of a pool of Cyclin E (Matsumoto and Maller, 2004; Ferguson and Maller, 2010). We speculate that Golgi-associated RhoBTB3$^{CUL3/RBX1}$ may locally regulate Cyclin E levels during S phase to prevent centrosome over-duplication (Fig. S2 C), which may trigger genomic instability (D'Assoro et al., 2002; Duensing, 2005; Koutsami et al., 2006).

Golgi localization is required for proper RhoBTB3 function. We have shown that RhoBTB3 is a peripheral Golgi protein that is likely to be responsible for the recruitment of a CUL3–ubiquitin ligase complex. Membrane recruitment regulates Ras family proteins in important ways (Colicelli, 2004; Pfeffer and Aivazian, 2004). Membrane association of Ras family members relies on two biochemical properties: the bound nucleotide-determined conformation of the protein and the presence of a lipidated C terminus. In contrast, RhoBTB3's Golgi-targeting domain lacks both nucleotide-binding capacity and its CAAX prenylation motif (Fig. 8 A). It is likely that RhoBTB3's Golgi association is mediated by an additional, yet to be identified, Golgi component.

Cyclin E intensity (C) were obtained using an unbiased quantification method (see Materials and methods). Data represent the mean of three independent experiments in which a total of >1,000 cells were analyzed in control and RhoBTB3 siRNA conditions, or ≥398 cells in rescue conditions. *t* test; *, P < 0.05; **, P < 0.01; error bars represent SEM. (D and E) Interaction of WT-RhoBTB3 or 1–525 RhoBTB3 construct with FLAG–Cyclin E (D) and FLAG-CUL3 (E) in total lysates from HEK293T cells. Cells were transfected as indicated at the top, immunoprecipitated with anti-FLAG antibody, and bound proteins were detected by immunoblot with antibodies to the proteins indicated at the right. Molecular mass marker mobility is shown at the left in kilodaltons. (F) HeLa cells were treated with indicated siRNA for a total of 72 h. At 24 h after siRNA, cells were transfected with plasmid encoding siRNA-resistant Myc-tagged WT-RhoBTB3 (top) or Myc-tagged 1–525 truncation (bottom). Left, Golgi structure assessed using mouse anti-GCC185. Middle, RhoBTB3 rescue construct expression detected using chicken anti-Myc. Right, TRITC-labeled siRNA. Asterisks are as in A above. Bars, 40 µm. (G and H) Quantification of Golgi fragmentation (G) and cell area (H). Color code as in B. Data in G and H represent the mean of four independent datasets in which a total of 150–200 cells were analyzed in all conditions. *t* test; *, P < 0.05; **, P < 0.01; ***, P < 0.001; error bars represent SEM.

Published October 21, 2013

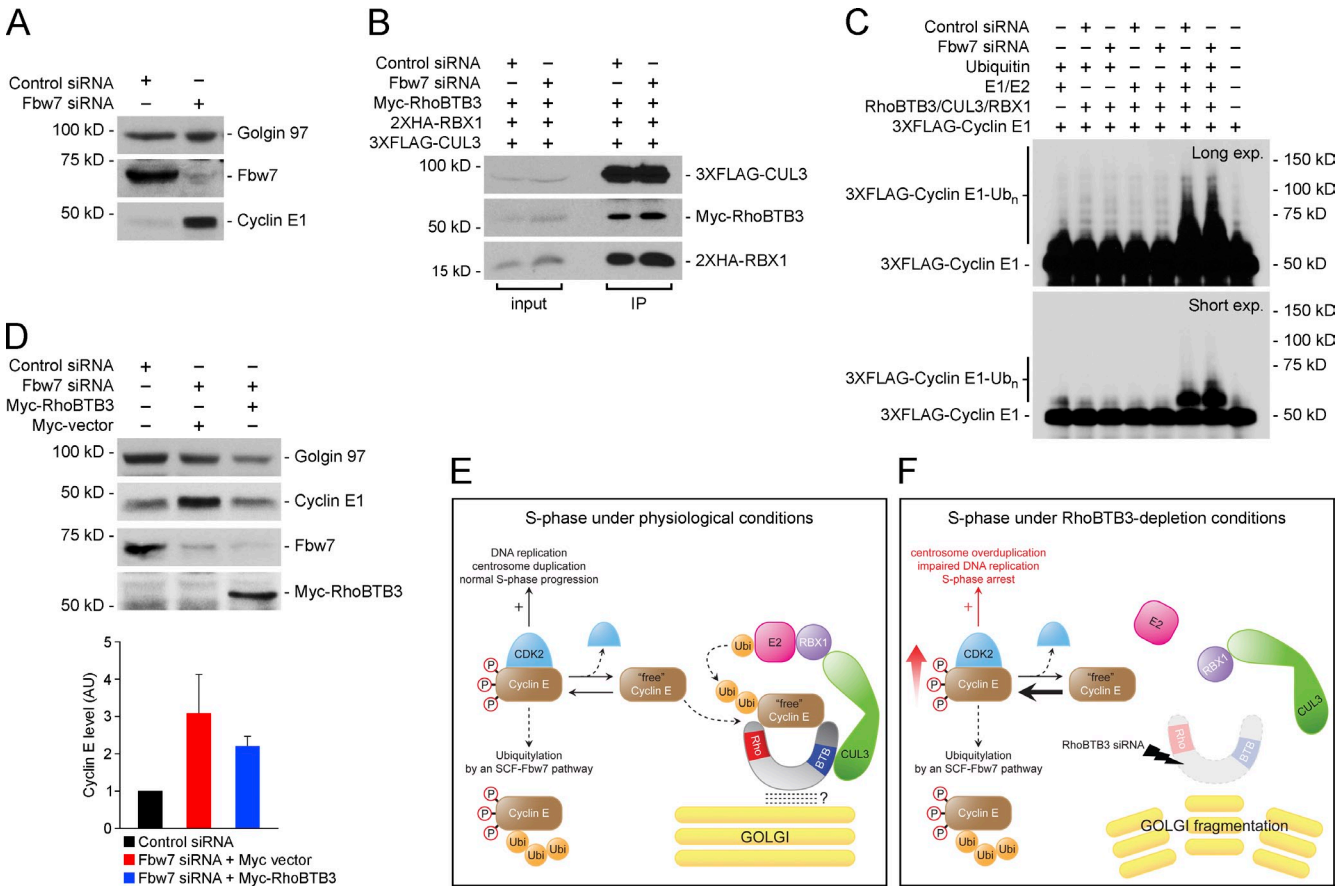

Figure 10. **RhoBTB3–CUL3 represents an alternative pathway for Cyclin E ubiquitylation.** (A) Fbw7 depletion in HEK293T cells assayed by immunoblot. Cyclin E1 increases after 72 h of Fbw7 siRNA treatment; Golgin 97 was used as a loading control. (B) Characterization of anti-FLAG immunopurified complexes containing Myc-RhoBTB3, FLAG-CUL3, and HA-RBX1 proteins in HEK293T cells treated either with control or Fbw7 siRNA. (C) In vitro–reconstituted ubiquitylation of Cyclin E using complexes shown in B. Top panel represents a long exposure of the same gel shown below (blotted using anti–Cyclin E). (D) Immunoblot detection of Cyclin E1 levels in HeLa cells treated with control (first lane) or Fbw7-siRNA (second and third lanes). After 24 h, cells were transfected either with Myc-empty vector (second lane) or Myc-RhoBTB3 (third lane); after 72 h total, extracts were analyzed as indicated. Overexpression of RhoBTB3 was detected using anti-Myc antibody; Golgin 97 was a loading control. Graph below shows mean Cyclin E levels from at least two independent experiments; error bars represent SEM. Molecular mass marker mobility is shown at left (A, B, and D) or right (C) in kilodaltons. (E and F) Model for RhoBTB3-mediated ubiquitylation of Cyclin E on the Golgi. Under physiological conditions (E), Golgi-associated RhoBTB3 binds to free Cyclin E and presents it to a CUL3–ubiquitin ligase for modification. Cyclin E can also be ubiquitylated by an SCF–Fbw7 pathway. Upon RhoBTB3 depletion (F), Cyclin E accumulates and Golgi fragmentation is observed.

Depletion or overexpression of RhoBTB3 has a profound effect on Golgi structure. Previous studies have demonstrated important roles for ubiquitylation and deubiquitylation in Golgi structure homeostasis (Meyer et al., 2002; Tang et al., 2011). For example, the AAA ATPase, p97, is important for the formation and maintenance of elongated Golgi cisternae (Uchiyama et al., 2006) and binds directly to ubiquitin conjugates via specific adaptor proteins (Meyer et al., 2002). p97 is thought to separate ubiquitinated substrates from tightly bound partner proteins throughout the cell cycle (Ye, 2006). In addition to binding Cyclin E directly, RhoBTB3's ATPase activity may play a role similar to p97 in untangling ubiquitylated protein complexes.

We have shown that CUL3 depletion also results in Golgi fragmentation, which implies that CUL3-dependent ubiquitylation is required for Golgi structure maintenance. p97 interacts indirectly with CUL3 to control ubiquitylation of specific substrates (den Besten et al., 2012). As a CUL3 adaptor protein, RhoBTB3 likely catalyzes ubiquitylation of proteins important for Golgi structure that may include p97. A parallel, Golgi-associated CUL7-dependent pathway also influences Golgi structure by ubiquitylation of GRASP65 protein (Litterman et al., 2011).

Previous studies have shown that interferon-γ signaling can up-regulate RhoBTB3 gene expression, concomitant with Cyclin E down-regulation (Amrani et al., 2003; Indraccolo et al., 2007). *RhoBTB3* is also up-regulated during S phase (Fig. 7 D; and www.cyclebase.org), consistent with its role in regulating Cyclin E levels. As is true for other Cullin-based ubiquitin ligase substrate adaptors, it is likely that RhoBTB3 targets multiple substrates (in addition to Cyclin E). Identification of the full range of RhoBTB3 substrates should provide additional mechanistic insight into how RhoBTB3 coordinates cell cycle progression, membrane trafficking, and Golgi homeostasis.

Mutations or overexpression of Ras oncogenes play an important role in human cancer development and progression (Malumbres and Barbacid, 2003). A number of Ras-related Rho GTPases have also been implicated in tumorigenesis (Sahai and Marshall, 2002). The classical function of Rho GTPases is regulation of the actin cytoskeleton (Jaffe and Hall, 2005). However,

Published October 21, 2013

Rho GTPases are also involved in other cellular processes including cell proliferation, and deregulation of their functions has been reported in cancer (Sahai and Marshall, 2002). Down-regulation of RhoBTB3 has been reported in different types of cancer (Berthold et al., 2008a), but the physiological consequences of this phenomenon and the underlying mechanisms remain unknown. Interestingly, mutations in RhoBTB3 have also been identified in several cancer cell lines and in tumors (Forbes et al., 2006); the mutations localize to the Rho domain (D72H; R87Q) or to the Golgi localization domain (S321Y; D360Y; S587L). It will be of interest to test the functional consequences of mutations at these positions.

Multiple Cullin–ubiquitin ligase pathways that target a common cyclin (including Cyclin E) have been described (Hwang and Clurman, 2005; Alao, 2007). For example, Cyclin D down-regulation is controlled primarily by a CUL1-dependent pathway (Lin et al., 2006), but an alternative CUL7-mediated pathway has also been reported (Paradis et al., 2013). Each of these pathways may be triggered upon specific upstream signals or may be compartmentalized in specific subcellular locations to regulate the abundance of distinct substrate pools. Thus, while the SCF-Fbw7 pathway mediates ubiquitylation of phosphorylated Cyclin E in the nucleolus (Bhaskaran et al., 2013), it appears that Golgi-associated RhoBTB3-CUL3 targets a different pool of Cyclin E that is unphosphorylated.

In the SCF ubiquitylation pathway, mutations in, or down-regulation of Fbw7 result in defective proteolysis and up-regulation of Cyclin E, which is implicated in oncogenesis (Hwang and Clurman, 2005; Welcker and Clurman, 2008). Indeed, high Cyclin E levels portend a poor prognosis in breast cancer (Enders, 2002; Keyomarsi et al., 2002). Our work suggests that down-regulation or mutations in RhoBTB3 may facilitate tumorigenesis by decreasing Cyclin E ubiquitylation and its subsequent degradation. Thus, RhoBTB3 may function as a tumor suppressor that regulates cell cycle progression by controlling Cyclin E levels as a substrate adaptor for a CUL3–ubiquitin ligase complex.

Why is Cyclin E regulation linked to the Golgi? Proliferating cells must grow past a certain cell size threshold in order to enter S phase (Jorgensen and Tyers, 2004). During active cell growth in G1, the Golgi plays an important role as a source of de novo membrane supply to increase the cell surface, which is a limiting factor for cell growth (McCusker and Kellogg, 2012). Therefore, it is possible that Golgi-mediated secretion is coupled to cell cycle progression at early stages of the cell cycle. In this context, RhoBTB3 may participate in sensing when the cell size threshold has been reached, and then target Cyclin E and other Golgi substrates for modification. In summary, these findings provide new detail to an unexpectedly Golgi-templated ubiquitylation pathway that contributes to the regulation of S phase of the mammalian cell cycle.

Materials and methods

Plasmids

The expression construct for RhoBTB3 with an N-terminal Myc tag was described previously (Espinosa et al., 2009). Full-length RhoBTB3 was amplified and ligated into pEGFP-C1 (Takara Bio Inc.) and into a modified pCS2+ vector (Invitrogen) containing a 3XFLAG tag at the N terminus (pCS2-3XFLAG). Site-directed mutagenesis was used to generate Myc-tagged RhoBTB3 truncations (Fig. 5 A). Cyclin E1 was amplified by PCR from a pCS2-Cyclin E1 expression vector (from M. Nachury, Stanford University, Stanford, CA) and ligated into pEGFP-N1 (Takara Bio Inc.), pCS2-3XFLAG, and a modified pcDNA3 vector (Invitrogen) with an N-terminal Myc tag (pcDNA3-Myc). Cyclin A2 was amplified by PCR from a pcDNA3-Ha-Cyclin A2 expression vector (gift of M. Nachury) and ligated into pEGFP-N1 (Takara Bio Inc.) and pcDNA3-Myc. Cyclin B1-YFP and CDK2-HA constructs were provided by J. Ferrell and D. Felsher (Stanford University, Stanford, CA), respectively. p3XFLAG-CUL3 was a gift of J. Roberts (Fred Hutchinson Cancer Research Center, Seattle, WA) and pEF-HA-Ubiquitin was from Z. Chen (University of Texas Southwestern, Dallas, TX). Myc-GRASP55 construct was provided by V. Malhotra (Centre for Genomic Regulation, Barcelona, Spain). The 2XHA-RBX1 construct was purchased from Addgene.

Cell culture and transfections

HeLa, HEK293T, and U2OS cells were grown in DMEM containing 10% fetal calf serum (FCS), antibiotics, and glutamine. DMEM and FCS were purchased from Invitrogen. Transient transfection was performed using Fugene 6 (Promega) or polyethyleneimine (Polysciences) for experiments using HeLa or HEK293T cells, respectively. Cells were used 12–48 h after transfection. All siRNAs were transfected using Dharmafect (Thermo Fisher Scientific) for 24, 48, or 72 h, as indicated. For transfection of constructs after siRNA treatment, cells were transfected usually 24 or 48 h after siRNA addition.

Antibodies and siRNAs

Antibodies were purchased as follows: rabbit anti-RhoBTB3 (Proteintech Group) requires blocking in 5% BSA-TBST; mouse anti-Myc (clone 9e10); chicken anti-Myc (Bethyl Laboratories, Inc.); mouse anti-FLAG (Sigma-Aldrich); rabbit anti-HA (Abcam); mouse anti–Cyclin E (BD) was used for immunoblotting; mouse monocolonal anti–Cyclin E (clone HE12; Santa Cruz Biotechnology, Inc.) was used for immunofluorescence; rabbit anti–Cyclin A2, –Cyclin B1, and mouse anti-ubiquitin (Santa Cruz Biotechnology, Inc.); mouse anti-Rb (from J. Sage, Stanford University, Stanford, CA); rabbit anti–phospho-Rb (GeneScript); rabbit anti-GFP (Invitrogen); mouse anti–α-tubulin and anti–γ-tubulin (Sigma-Aldrich); rabbit anti-GCC185 (Reddy et al., 2006); anti-GM130 (BD); and rabbit anti-Fbw7 (Novus Biologicals). A small recombinant His-tagged, 13-kD GFP-binding protein comprising the epitope recognition domain of a single, heavy chain antibody raised in an alpaca against GFP was purified (Rothbauer et al., 2008). Sequences of siRNAs used were: control, 5′-GUUCAAUAGGCUUACUAAUUU-3′; RhoBTB3 #1, 5′-AGGAAGAAGUUGAAAGAUUUU-3′ (for experiments in Figs. 1, 2, 6, 7, 8, S1, S2, and S3); RhoBTB3 #2, 5′-GGGAAGAAUUGGAAGAAGAUU-3′ (for experiments in Figs. 2, 7 and S2); TRITC-RhoBTB3 siRNA (Espinosa et al., 2009; for experiments in Figs. 1 and S1); Cyclin E1 siRNA, 5′-CAGCCAAACUUGAGGAAAUUU-3′; CUL3, 5′-GGUGAUGAUUAGAGACAUAUU-3′; and siRNA for Fbw7 exon 10 (van Drogen et al., 2006). All siRNAs were transfected using Dharmafect (Thermo Fisher Scientific) for 48 or 72 h, as indicated. For transfection of constructs after siRNA treatment, cells were transfected usually 24 or 48 h after siRNA addition.

Microscopy and data analysis

For immunofluorescence, cells grown on coverslips were fixed with 3.7% paraformaldehyde or with 100% methanol at −20°C (for anti–γ-tubulin or anti–Cyclin E). After this, cells were permeabilized with 0.1% Triton X-100, and blocked with 1% BSA in PBS for 15 min at 37°C. Cells were incubated with the indicated primary antibodies, subsequently with secondary antibodies labeled with Alexa Fluor 488, 594, or 647 (Molecular Probes) or Cy5 (Jackson ImmunoResearch Laboratories. Inc.), and finally coverslips were mounted with Mowiol (EMD Millipore). Confocal images were acquired at room temperature using a confocal scanner (TCS SP2 SE; Leica) in conjunction with an upright scope (DM6000 B; Leica) with an HCX PL Apochromatic 63×/NA 1.4 objective (Leica), a confocal control box (CTR 6000; Leica), and Leica Control software. Unbiased, automatic quantifications of images (Fig. 6, B and C; Fig. S1 C) were performed with CellProfiler 2.0 software. For nuclear Cyclin E quantification, nuclear regions were identified by DAPI, and integrated fluorescence intensity and nuclear area were determined. Statistical analysis was conducted by a Student's *t* test. In some rescue experiments (Fig. 6 H), cell area was measured using ImageJ (National Institutes of Health). Finally, Golgi fragmentation was scored visually and results were normalized to the control condition. For in vivo video microscopy, cells treated for 48 h with either control or RhoBTB3

Published October 21, 2013

#1 siRNA were imaged every 3.5 min for 15 h using an inverted microscope (Axio Observer Z1; Carl Zeiss) fitted with an LD Plan-Neofluar 20×/0.4 Korr Ph1 Ph2 objective and a CCD camera (AxioCam MRm; Carl Zeiss) controlled by Axiovision 4.8 software (Carl Zeiss). The microscope was equipped with an incubation system with 37°C temperature and CO_2 control. Data were analyzed with ImageJ.

Flow cytometry

HeLa cells were treated with either control or RhoBTB3 #1 siRNA. After 24, 48, and 72 h cells were harvested and washed before fixation in 70% ethanol. After this, cells were washed and stained with a phosphate-buffered saline (PBS) solution containing 50 µg/ml propidium iodide (PI) and 100 µg/ml propidium RNase A. Cells were assayed on a FACS analyzer (FACScan; BD) and data were analyzed using Flowjo software (Tree Star).

Immunoprecipitations

HEK293T cells overexpressing indicated constructs were harvested after 12–36 h and lysed in lysis buffer (50 mM Hepes, pH 7.4, 150 mM NaCl, 5 mM $MgCl_2$, and 1% Triton X-100) supplemented with protease inhibitors. After centrifugation at 12,000 *g* for 10 min, protein concentrations were measured in the lysates. Equal amounts of extracts were precleared with protein A–Sepharose beads (GE Healthcare) at 4°C for 30 min. The precleared extracts were incubated with either GFP-binding protein–conjugated agarose or anti-FLAG antibody-conjugated agarose for 1–2 h at 4°C. Immobilized proteins were washed with lysis buffer, eluted with 2× Laemmli buffer, and subjected to SDS-PAGE. For immunoprecipitations using membrane fractions, cells were swollen in hypotonic buffer (10 mM Hepes, pH 7.4) for 10 min on ice. Immediately after this, cells were homogenized by 15 passages through a 25-gauge needle in cold homogenization buffer (10 mM Hepes, pH 7.4, 150 mM KCl, 5 mM $MgCl_2$, 1 mM EDTA, and 1 mM ATP) supplemented with protease inhibitors. Cell homogenates were then spun at 800 *g* for 5 min at 4°C to obtain a post-nuclear supernatant (PNS) fraction. Next, PNS fractions were centrifuged at 100,000 *g* at 4°C to pellet membranes. Membrane fractions were solubilized in cold homogenization buffer containing 1% Triton X-100. After this, membrane extracts were used as described above. In some experiments (Fig. 3 A), bands from immunoprecipitation blots were quantified using ImageJ, and data were analyzed by a Student's *t* test.

Protein expression and purification of recombinant proteins

GST–Cyclin E was expressed and purified as the binary complex but without detergent. For purification of a CUL3–RBX1 binary complex, GST-CUL3 and 2HA-RBX constructs were co-transformed into BL21 (DE3) Rosetta II cells and cultures (OD_{600} = 0.6) were induced with 0.1 mM IPTG for 18 h at 16°C. Cells were resuspended in 50 mM Hepes, pH 7.4, 300 mM NaCl, 1 mM DTT, 5 mM $MgCl_2$, 0.5% Triton X-100, and full protease inhibitor cocktail and lysed by two passes at >10,000 lb/in^2 in an EmulsiFlex-C5 apparatus (Avestin). Lysates were clarified by centrifugation twice at 20,000 rpm for 20 min each in a rotor (JA 20; Beckman Coulter). Clarified lysates were incubated with glutathione 4B–Sepharose beads (GE Healthcare) for 1 h at 4°C, washed with 50 vol of 50 mM Hepes, pH 7.4, 300 mM NaCl, 1 mM DTT, and 5 mM $MgCl_2$, and eluted with 50 mM Hepes, pH 7.4, 300 mM NaCl, 1 mM DTT, 5 mM $MgCl_2$, and 20 mM glutathione. For in vitro reconstitution of RhoBTB3–CUL3–RBX1 complexes, a FLAG-RhoBTB3 construct was transformed into BL21 (DE3) Rosetta II cells, and cultures (OD_{600} = 0.6) were induced with 0.1 mM IPTG for 18 h at 16°C. Cells were resuspended in 50 mM Hepes, pH 7.4, 300 mM NaCl, 1 mM DTT, 5 mM $MgCl_2$, 0.5% Triton X-100, and full protease inhibitor cocktail and lysed by two passes at >10,000 lb/in^2 in an EmulsiFlex-C5 apparatus (Avestin). Lysates were clarified by centrifugation twice at 20,000 rpm for 20 min each in a rotor (JA 20; Beckman Coulter). Clarified lysates were incubated with anti-FLAG M2 antibody–conjugated agarose (Sigma-Aldrich) for 2 h at 4°C, and then washed with 50 vol of 50 mM Hepes, pH 7.4, 300 mM NaCl, 1 mM DTT, and 5 mM $MgCl_2$. After this, excess CUL3–RBX1 binary complex was mixed with purified FLAG-RhoBTB3 bound to anti-FLAG antibody–conjugated agarose for 90 min at 4°C followed by a 50-vol wash with 50 mM Hepes, pH 7.4, 300 mM NaCl, 1 mM DTT, and 5 mM $MgCl_2$ to remove unbound CUL3–RBX1. Finally, RhoBTB3–CUL3–RBX1 ternary complexes were eluted with 50 mM Tris-HCl, pH 7.5, 50 mM NaCl, 1 mM DTT, 1 mM $MgCl_2$, and 0.2 mg/ml FLAG peptide (Sigma-Aldrich). Stoichiometry of purified binary and ternary complexes was analyzed by SDS-PAGE, Coomassie blue staining, and immunoblotting. Proteins were stored on ice.

Isolation of mammalian RhoBTB3$^{CUL3/RBX1}$ complexes

RhoBTB3–CUL3–RBX1 complex was purified using anti-FLAG M2 agarose beads (Sigma-Aldrich) from lysates of HEK293T cells transfected with FLAG-CUL3, Myc-RhoBTB3, and 2XHA-ROC1. RhoBTB3-deficient complexes were immunopurified from HEK293T cells transfected with FLAG-CUL3 and 2XHA-RBX1 and treated with RhoBTB3 siRNA (#1 and #2) for 72 h. Complexes bound on beads were eluted by incubation with FLAG peptide (Sigma-Aldrich) overnight. Human FLAG–Cyclin E1 was also purified from HEK293T cells as described above. Relative yields of both complexes and Cyclin E immunopurifications were analyzed by immunoblotting.

In vitro ubiquitylation assay

Purified GST–Cyclin E and complexes were incubated at 30°C for 1 h in a 40-µl reaction mixture containing 50 mM Tris-HCl, pH 7.5, 1 mM $MgCl_2$, 0.5 µg/µL ubiquitin, 2 µM ubiquitin aldehyde, 10 µM MG132, 1 mM ATP, 2 mM NaF, 1 mM DTT, 7.5 mM creatine phosphate, 40 mU/µL creatine phospho-kinase, 2 ng/µL yeast E1, and 20 ng/µL E2 (UbcH5a). All ubiquitin-related reagents were purchased from Boston Biochemicals. For reactions performed with bacterially expressed components, complexes were added at 100 nM based on Cullin 3 concentration.

Online supplemental material

Fig. S1 shows increased nuclear size and micronuclei number upon RhoBTB3 depletion. Fig. S2 shows that Cyclin E1 increases upon depletion of RhoBTB3. Fig. S3 shows that overexpression of CDK2 with Cyclin E1 or Myc-RhoBTB3 causes Golgi fragmentation, and depletion of either Cyclin E1 or RhoBTB3 causes Golgi disruption. Fig. S4 shows that CUL3 depletion leads to Golgi fragmentation and enlarged cell/nuclear size. Fig. S5 shows the subcellular distribution of Cyclin E in HeLa or HEK293T cells, before or after transfection with Cyclin E1. Video 1 shows time-lapse phase-contrast video microscopy of HeLa cells after 48 h with control or RhoBTB3 siRNA. Online supplemental material is available at http://www.jcb.org/cgi/content/full/jcb.201305158/DC1.

We thank Aaron Straight for advice and encouragement and Jim Ferrell and James Roberts for constructs.

This research was funded by a grant to S.R. Pfeffer from the National Institutes of Health (DK37332).

Author contributions: A. Lu designed and performed all experiments, analyzed data and wrote the paper; S.R. Pfeffer provided advice and co-wrote the paper.

Submitted: 31 May 2013
Accepted: 11 September 2013

References

Alao, J.P. 2007. The regulation of cyclin D1 degradation: roles in cancer development and the potential for therapeutic invention. *Mol. Cancer*. 6:24. http://dx.doi.org/10.1186/1476-4598-6-24

Amrani, Y., O. Tliba, D. Choubey, C.D. Huang, V.P. Krymskaya, A. Eszterhas, A.L. Lazaar, and R.A. Panettieri Jr. 2003. IFN-gamma inhibits human airway smooth muscle cell proliferation by modulating the E2F-1/Rb pathway. *Am. J. Physiol. Lung Cell. Mol. Physiol.* 284:L1063–L1071.

Bennett, E.J., J. Rush, S.P. Gygi, and J.W. Harper. 2010. Dynamics of cullin-RING ubiquitin ligase network revealed by systematic quantitative proteomics. *Cell*. 143:951–965. http://dx.doi.org/10.1016/j.cell.2010.11.017

Berthold, J., K. Schenková, S. Ramos, Y. Miura, M. Furukawa, P. Aspenström, and F. Rivero. 2008a. Characterization of RhoBTB-dependent Cul3 ubiquitin ligase complexes—evidence for an autoregulatory mechanism. *Exp. Cell Res.* 314:3453–3465. http://dx.doi.org/10.1016/j.yexcr.2008.09.005

Berthold, J., K. Schenkova, and F. Rivero. 2008b. Rho GTPases of the RhoBTB subfamily and tumorigenesis. *Acta Pharmacol. Sin.* 29:285–295. http://dx.doi.org/10.1111/j.1745-7254.2008.00773.x

Bhaskaran, N., F. van Drogen, H.F. Ng, R. Kumar, S. Ekholm-Reed, M. Peter, O. Sangfelt, and S.I. Reed. 2013. Fbw7α and Fbw7γ collaborate to shuttle cyclin E1 into the nucleolus for multiubiquitylation. *Mol. Cell. Biol.* 33:85–97. http://dx.doi.org/10.1128/MCB.00288-12

Colanzi, A., C. Suetterlin, and V. Malhotra. 2003. Cell-cycle-specific Golgi fragmentation: how and why? *Curr. Opin. Cell Biol.* 15:462–467. http://dx.doi.org/10.1016/S0955-0674(03)00067-X

Colicelli, J. 2004. Human RAS superfamily proteins and related GTPases. *Sci. STKE*. 2004:RE13.

D'Assoro, A.B., W.L. Lingle, and J.L. Salisbury. 2002. Centrosome amplification and the development of cancer. *Oncogene*. 21:6146–6153. http://dx.doi.org/10.1038/sj.onc.1205772

den Besten, W., R. Verma, G. Kleiger, R.S. Oania, and R.J. Deshaies. 2012. NEDD8 links cullin-RING ubiquitin ligase function to the p97 pathway. *Nat. Struct. Mol. Biol.* 19:511–516: S1. http://dx.doi.org/10.1038/nsmb.2269

Draviam, V.M., S. Orrechia, M. Lowe, R. Pardi, and J. Pines. 2001. The localization of human cyclins B1 and B2 determines CDK1 substrate specificity and neither enzyme requires MEK to disassemble the Golgi apparatus. *J. Cell Biol.* 152:945–958. http://dx.doi.org/10.1083/jcb.152.5.945

Duensing, S. 2005. A tentative classification of centrosome abnormalities in cancer. *Cell Biol. Int.* 29:352–359. http://dx.doi.org/10.1016/j.cellbi.2005.03.005

Dulić, V., E. Lees, and S.I. Reed. 1992. Association of human cyclin E with a periodic G1-S phase protein kinase. *Science*. 257:1958–1961. http://dx.doi.org/10.1126/science.1329201

Ekholm, S.V., P. Zickert, S.I. Reed, and A. Zetterberg. 2001. Accumulation of cyclin E is not a prerequisite for passage through the restriction point. *Mol. Cell. Biol.* 21:3256–3265. http://dx.doi.org/10.1128/MCB.21.9.3256-3265.2001

Enders, G.H. 2002. Cyclins in breast cancer: too much of a good thing. *Breast Cancer Res.* 4:145–147. http://dx.doi.org/10.1186/bcr439

Errico, A., K. Deshmukh, Y. Tanaka, A. Pozniakovsky, and T. Hunt. 2010. Identification of substrates for cyclin dependent kinases. *Adv. Enzyme Regul.* 50:375–399. http://dx.doi.org/10.1016/j.advenzreg.2009.12.001

Espinosa, E.J., M. Calero, K. Sridevi, and S.R. Pfeffer. 2009. RhoBTB3: a Rho GTPase-family ATPase required for endosome to Golgi transport. *Cell*. 137:938–948. http://dx.doi.org/10.1016/j.cell.2009.03.043

Ferguson, R.L., and J.L. Maller. 2010. Centrosomal localization of cyclin E-Cdk2 is required for initiation of DNA synthesis. *Curr. Biol.* 20:856–860. http://dx.doi.org/10.1016/j.cub.2010.03.028

Forbes, S., J. Clements, E. Dawson, S. Bamford, T. Webb, A. Dogan, A. Flanagan, J. Teague, R. Wooster, P.A. Futreal, and M.R. Stratton. 2006. Cosmic 2005. *Br. J. Cancer*. 94:318–322. http://dx.doi.org/10.1038/sj.bjc.6602928

Furukawa, M., Y.J. He, C. Borchers, and Y. Xiong. 2003. Targeting of protein ubiquitination by BTB-Cullin 3-Roc1 ubiquitin ligases. *Nat. Cell Biol.* 5:1001–1007. http://dx.doi.org/10.1038/ncb1056

Gaulin, J.F., A. Fiset, S. Fortier, and R.L. Faure. 2000. Characterization of Cdk2-cyclin E complexes in plasma membrane and endosomes of liver parenchyma. Insulin-dependent regulation. *J. Biol. Chem.* 275:16658–16665. http://dx.doi.org/10.1074/jbc.275.22.16658

Geng, Y., Q. Yu, E. Sicinska, M. Das, J.E. Schneider, S. Bhattacharya, W.M. Rideout, R.T. Bronson, H. Gardner, and P. Sicinski. 2003. Cyclin E ablation in the mouse. *Cell*. 114:431–443. http://dx.doi.org/10.1016/S0092-8674(03)00645-7

Geng, Y., Y.M. Lee, M. Welcker, J. Swanger, A. Zagozdzon, J.D. Winer, J.M. Roberts, P. Kaldis, B.E. Clurman, and P. Sicinski. 2007. Kinase-independent function of cyclin E. *Mol. Cell*. 25:127–139. http://dx.doi.org/10.1016/j.molcel.2006.11.029

Hao, B., S. Oehlmann, M.E. Sowa, J.W. Harper, and N.P. Pavletich. 2007. Structure of a Fbw7-Skp1-cyclin E complex: multisite-phosphorylated substrate recognition by SCF ubiquitin ligases. *Mol. Cell*. 26:131–143. http://dx.doi.org/10.1016/j.molcel.2007.02.022

Hengst, L., V. Dulic, J.M. Slingerland, E. Lees, and S.I. Reed. 1994. A cell cycle-regulated inhibitor of cyclin-dependent kinases. *Proc. Natl. Acad. Sci. USA*. 91:5291–5295. http://dx.doi.org/10.1073/pnas.91.12.5291

Hwang, H.C., and B.E. Clurman. 2005. Cyclin E in normal and neoplastic cell cycles. *Oncogene*. 24:2776–2786. http://dx.doi.org/10.1038/sj.onc.1208613

Indraccolo, S., U. Pfeffer, S. Minuzzo, G. Esposito, V. Roni, S. Mandruzzato, N. Ferrari, L. Anfosso, R. Dell'Eva, D.M. Noonan, et al. 2007. Identification of genes selectively regulated by IFNs in endothelial cells. *J. Immunol.* 178:1122–1135.

Jaffe, A.B., and A. Hall. 2005. Rho GTPases: biochemistry and biology. *Annu. Rev. Cell Dev. Biol.* 21:247–269. http://dx.doi.org/10.1146/annurev.cellbio.21.020604.150721

Jorgensen, P., and M. Tyers. 2004. How cells coordinate growth and division. *Curr. Biol.* 14:R1014–R1027. http://dx.doi.org/10.1016/j.cub.2004.11.027

Keyomarsi, K., S.L. Tucker, T.A. Buchholz, M. Callister, Y. Ding, G.N. Hortobagyi, I. Bedrosian, C. Knickerbocker, W. Toyofuku, M. Lowe, et al. 2002. Cyclin E and survival in patients with breast cancer. *N. Engl. J. Med.* 347:1566–1575. http://dx.doi.org/10.1056/NEJMoa021153

Koepp, D.M., L.K. Schaefer, X. Ye, K. Keyomarsi, C. Chu, J.W. Harper, and S.J. Elledge. 2001. Phosphorylation-dependent ubiquitination of cyclin E by the SCFFbw7 ubiquitin ligase. *Science*. 294:173–177. http://dx.doi.org/10.1126/science.1065203

Koff, A., A. Giordano, D. Desai, K. Yamashita, J.W. Harper, S. Elledge, T. Nishimoto, D.O. Morgan, B.R. Franza, and J.M. Roberts. 1992. Formation and activation of a cyclin E-cdk2 complex during the G1 phase of the human cell cycle. *Science*. 257:1689–1694. http://dx.doi.org/10.1126/science.1388288

Koutsami, M.K., P.K. Tsantoulis, M. Kouloukoussa, K. Apostolopoulou, I.S. Pateras, Z. Spartinou, A. Drougou, K. Evangelou, C. Kittas, J. Bartkova, et al. 2006. Centrosome abnormalities are frequently observed in non-small-cell lung cancer and are associated with aneuploidy and cyclin E overexpression. *J. Pathol.* 209:512–521. http://dx.doi.org/10.1002/path.2005

Krek, W. 2003. BTB proteins as henchmen of Cul3-based ubiquitin ligases. *Nat. Cell Biol.* 5:950–951. http://dx.doi.org/10.1038/ncb1103-950

Lee, H.O., J.M. Davidson, and R.J. Duronio. 2009. Endoreplication: polyploidy with purpose. *Genes Dev.* 23:2461–2477. http://dx.doi.org/10.1101/gad.1829209

Lin, D.I., O. Barbash, K.G. Kumar, J.D. Weber, J.W. Harper, A.J. Klein-Szanto, A. Rustgi, S.Y. Fuchs, and J.A. Diehl. 2006. Phosphorylation-dependent ubiquitination of cyclin D1 by the SCF(FBX4-alphaB crystallin) complex. *Mol. Cell*. 24:355–366. http://dx.doi.org/10.1016/j.molcel.2006.09.007

Litterman, N., Y. Ikeuchi, G. Gallardo, B.C. O'Connell, M.E. Sowa, S.P. Gygi, J.W. Harper, and A. Bonni. 2011. An OBSL1-Cul7Fbxw8 ubiquitin ligase signaling mechanism regulates Golgi morphology and dendrite patterning. *PLoS Biol.* 9:e1001060. http://dx.doi.org/10.1371/journal.pbio.1001060

Maerki, S., M.H. Olma, T. Staubli, P. Steigemann, D.W. Gerlich, M. Quadroni, I. Sumara, and M. Peter. 2009. The Cul3-KLHL21 E3 ubiquitin ligase targets aurora B to midzone microtubules in anaphase and is required for cytokinesis. *J. Cell Biol.* 187:791–800. http://dx.doi.org/10.1083/jcb.200906117

Malumbres, M., and M. Barbacid. 2003. RAS oncogenes: the first 30 years. *Nat. Rev. Cancer*. 3:459–465. http://dx.doi.org/10.1038/nrc1097

Matsumoto, Y., and J.L. Maller. 2004. A centrosomal localization signal in cyclin E required for Cdk2-independent S phase entry. *Science*. 306:885–888. http://dx.doi.org/10.1126/science.1103544

McCusker, D., and D.R. Kellogg. 2012. Plasma membrane growth during the cell cycle: unsolved mysteries and recent progress. *Curr. Opin. Cell Biol.* 24:845–851. http://dx.doi.org/10.1016/j.ceb.2012.10.008

McEvoy, J.D., U. Kossatz, N. Malek, and J.D. Singer. 2007. Constitutive turnover of cyclin E by Cul3 maintains quiescence. *Mol. Cell. Biol.* 27:3651–3666. http://dx.doi.org/10.1128/MCB.00720-06

Meyer, H.H., Y. Wang, and G. Warren. 2002. Direct binding of ubiquitin conjugates by the mammalian p97 adaptor complexes, p47 and Ufd1-Npl4. *EMBO J.* 21:5645–5652. http://dx.doi.org/10.1093/emboj/cdf579

Nacak, T.G., K. Leptien, D. Fellner, H.G. Augustin, and J. Kroll. 2006. The BTB-kelch protein LZTR-1 is a novel Golgi protein that is degraded upon induction of apoptosis. *J. Biol. Chem.* 281:5065–5071. http://dx.doi.org/10.1074/jbc.M509073200

Ohtsubo, M., A.M. Theodoras, J. Schumacher, J.M. Roberts, and M. Pagano. 1995. Human cyclin E, a nuclear protein essential for the G1-to-S phase transition. *Mol. Cell. Biol.* 15:2612–2624.

Pagliuca, F.W., M.O. Collins, A. Lichawska, P. Zegerman, J.S. Choudhary, and J. Pines. 2011. Quantitative proteomics reveals the basis for the biochemical specificity of the cell-cycle machinery. *Mol. Cell*. 43:406–417. http://dx.doi.org/10.1016/j.molcel.2011.05.031

Paradis, V., M. Albuquerque, M. Mebarki, L. Hernandez, S. Zalinski, S. Quentin, J. Belghiti, J. Soulier, and P. Bedossa. 2013. Cullin7: a new gene involved in liver carcinogenesis related to metabolic syndrome. *Gut*. 62:911–919. http://dx.doi.org/10.1136/gutjnl-2012-302091

Perez-Torrado, R., D. Yamada, and P.A. Defossez. 2006. Born to bind: the BTB protein-protein interaction domain. *Bioessays*. 28:1194–1202. http://dx.doi.org/10.1002/bies.20500

Persico, A., R.I. Cervigni, M.L. Barretta, D. Corda, and A. Colanzi. 2010. Golgi partitioning controls mitotic entry through Aurora-A kinase. *Mol. Biol. Cell*. 21:3708–3721. http://dx.doi.org/10.1091/mbc.E10-03-0243

Petroski, M.D., and R.J. Deshaies. 2005. Function and regulation of cullin-RING ubiquitin ligases. *Nat. Rev. Mol. Cell Biol.* 6:9–20. http://dx.doi.org/10.1038/nrm1547

Pfeffer, S., and D. Aivazian. 2004. Targeting Rab GTPases to distinct membrane compartments. *Nat. Rev. Mol. Cell Biol.* 5:886–896. http://dx.doi.org/10.1038/nrm1500

Pintard, L., J.H. Willis, A. Willems, J.L. Johnson, M. Srayko, T. Kurz, S. Glaser, P.E. Mains, M. Tyers, B. Bowerman, and M. Peter. 2003. The BTB protein MEL-26 is a substrate-specific adaptor of the CUL-3 ubiquitin-ligase. *Nature*. 425:311–316. http://dx.doi.org/10.1038/nature01959

Potemski, P., R. Kusinska, C. Watala, E. Pluciennik, A.K. Bednarek, and R. Kordek. 2006. Cyclin E expression in breast cancer correlates with negative steroid receptor status, HER2 expression, tumor grade and proliferation. *J. Exp. Clin. Cancer Res.* 25:59–64.

Preisinger, C., R. Körner, M. Wind, W.D. Lehmann, R. Kopajtich, and F.A. Barr. 2005. Plk1 docking to GRASP65 phosphorylated by Cdk1 suggests a mechanism for Golgi checkpoint signalling. *EMBO J.* 24:753–765. http://dx.doi.org/10.1038/sj.emboj.7600569

Rajagopalan, H., P.V. Jallepalli, C. Rago, V.E. Velculescu, K.W. Kinzler, B. Vogelstein, and C. Lengauer. 2004. Inactivation of hCDC4 can cause

chromosomal instability. *Nature*. 428:77–81. http://dx.doi.org/10.1038/nature02313

Reddy, J.V., A.S. Burguete, K. Sridevi, I.G. Ganley, R.M. Nottingham, and S.R. Pfeffer. 2006. A functional role for the GCC185 golgin in mannose 6-phosphate receptor recycling. *Mol. Biol. Cell*. 17:4353–4363. http://dx.doi.org/10.1091/mbc.E06-02-0153

Resnitzky, D., M. Gossen, H. Bujard, and S.I. Reed. 1994. Acceleration of the G1/S phase transition by expression of cyclins D1 and E with an inducible system. *Mol. Cell. Biol.* 14:1669–1679.

Rothbauer, U., K. Zolghadr, S. Muyldermans, A. Schepers, M.C. Cardoso, and H. Leonhardt. 2008. A versatile nanotrap for biochemical and functional studies with fluorescent fusion proteins. *Mol. Cell Proteomics*. 7:282–289. http://dx.doi.org/10.1074/mcp.M700342-MCP200

Sahai, E., and C.J. Marshall. 2002. RHO-GTPases and cancer. *Nat. Rev. Cancer*. 2:133–142. http://dx.doi.org/10.1038/nrc725

Santra, M.K., N. Wajapeyee, and M.R. Green. 2009. F-box protein FBXO31 mediates cyclin D1 degradation to induce G1 arrest after DNA damage. *Nature*. 459:722–725. http://dx.doi.org/10.1038/nature08011

Scaltriti, M., P.J. Eichhorn, J. Cortés, L. Prudkin, C. Aura, J. Jiménez, S. Chandarlapaty, V. Serra, A. Prat, Y.H. Ibrahim, et al. 2011. Cyclin E amplification/overexpression is a mechanism of trastuzumab resistance in HER2+ breast cancer patients. *Proc. Natl. Acad. Sci. USA*. 108:3761–3766. http://dx.doi.org/10.1073/pnas.1014835108

Singer, J.D., M. Gurian-West, B. Clurman, and J.M. Roberts. 1999. Cullin-3 targets cyclin E for ubiquitination and controls S phase in mammalian cells. *Genes Dev.* 13:2375–2387. http://dx.doi.org/10.1101/gad.13.18.2375

Siripurapu, V., J. Meth, N. Kobayashi, and M. Hamaguchi. 2005. DBC2 significantly influences cell-cycle, apoptosis, cytoskeleton and membrane-trafficking pathways. *J. Mol. Biol.* 346:83–89. http://dx.doi.org/10.1016/j.jmb.2004.11.043

Spruck, C.H., K.A. Won, and S.I. Reed. 1999. Deregulated cyclin E induces chromosome instability. *Nature*. 401:297–300. http://dx.doi.org/10.1038/45836

Sütterlin, C., P. Hsu, A. Mallabiabarrena, and V. Malhotra. 2002. Fragmentation and dispersal of the pericentriolar Golgi complex is required for entry into mitosis in mammalian cells. *Cell*. 109:359–369. http://dx.doi.org/10.1016/S0092-8674(02)00720-1

Tang, D., Y. Xiang, S. De Renzis, J. Rink, G. Zheng, M. Zerial, and Y. Wang. 2011. The ubiquitin ligase HACE1 regulates Golgi membrane dynamics during the cell cycle. *Nat Commun*. 2:501. http://dx.doi.org/10.1038/ncomms1509

Uchiyama, K., G. Totsukawa, M. Puhka, Y. Kaneko, E. Jokitalo, I. Dreveny, F. Beuron, X. Zhang, P. Freemont, and H. Kondo. 2006. p37 is a p97 adaptor required for Golgi and ER biogenesis in interphase and at the end of mitosis. *Dev. Cell*. 11:803–816. http://dx.doi.org/10.1016/j.devcel.2006.10.016

van Drogen, F., O. Sangfelt, A. Malyukova, L. Matskova, E. Yeh, A.R. Means, and S.I. Reed. 2006. Ubiquitylation of cyclin E requires the sequential function of SCF complexes containing distinct hCdc4 isoforms. *Mol. Cell*. 23:37–48. http://dx.doi.org/10.1016/j.molcel.2006.05.020

Welcker, M., and B.E. Clurman. 2008. FBW7 ubiquitin ligase: a tumour suppressor at the crossroads of cell division, growth and differentiation. *Nat. Rev. Cancer*. 8:83–93. http://dx.doi.org/10.1038/nrc2290

Willmarth, N.E., D.G. Albertson, and S.P. Ethier. 2004. Chromosomal instability and lack of cyclin E regulation in hCdc4 mutant human breast cancer cells. *Breast Cancer Res.* 6:R531–R539. http://dx.doi.org/10.1186/bcr900

Woo, R.A., and R.Y. Poon. 2003. Cyclin-dependent kinases and S phase control in mammalian cells. *Cell Cycle*. 2:316–324. http://dx.doi.org/10.4161/cc.2.4.468

Xu, L., Y. Wei, J. Reboul, P. Vaglio, T.H. Shin, M. Vidal, S.J. Elledge, and J.W. Harper. 2003. BTB proteins are substrate-specific adaptors in an SCF-like modular ubiquitin ligase containing CUL-3. *Nature*. 425:316–321. http://dx.doi.org/10.1038/nature01985

Ye, Y. 2006. Diverse functions with a common regulator: ubiquitin takes command of an AAA ATPase. *J. Struct. Biol.* 156:29–40. http://dx.doi.org/10.1016/j.jsb.2006.01.005

Zhang, F.L., and P.J. Casey. 1996. Protein prenylation: molecular mechanisms and functional consequences. *Annu. Rev. Biochem.* 65:241–269. http://dx.doi.org/10.1146/annurev.bi.65.070196.001325

Zheng, N., B.A. Schulman, L. Song, J.J. Miller, P.D. Jeffrey, P. Wang, C. Chu, D.M. Koepp, S.J. Elledge, M. Pagano, et al. 2002. Structure of the Cul1-Rbx1-Skp1-F boxSkp2 SCF ubiquitin ligase complex. *Nature*. 416:703–709. http://dx.doi.org/10.1038/416703a

Lu and Pfeffer, http://www.jcb.org/cgi/content/full/jcb.201305158/DC1

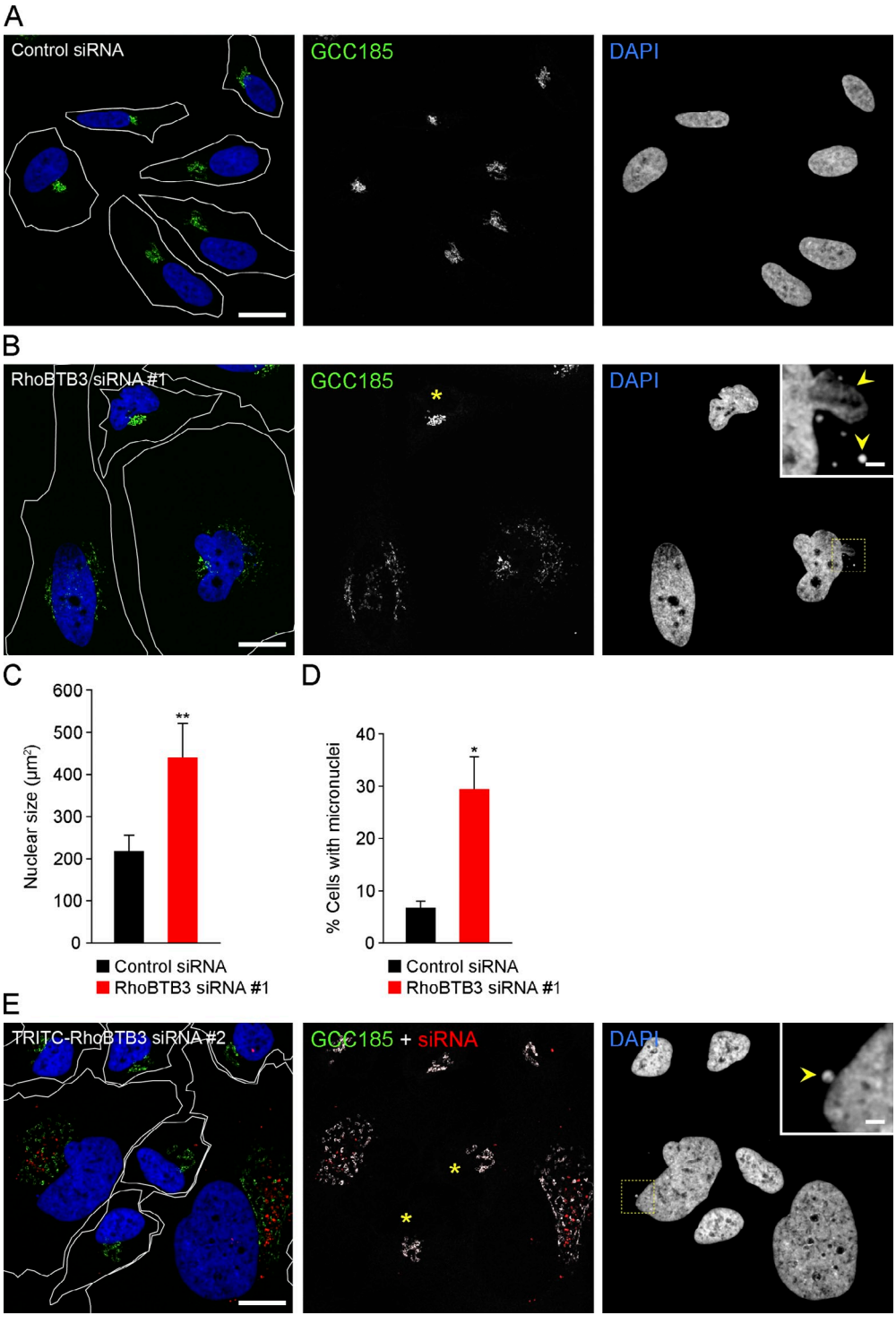

Figure S1. **siRNA depletion of RhoBTB3 increases nuclear size and induces micronuclei formation.** (A–E) RhoBTB3 depletion using two distinct siRNAs increases nuclear size and micronuclei number. siRNA depletion was for 72 h. Asterisks indicate nondepleted HeLa cells displaying a typical Golgi ribbon (detected with anti-GCC185 antibody) and "normal" cell and nuclear size. Arrowheads indicate presence of micronuclei in RhoBTB3-depleted cells. (C and D) Quantification of nuclear size and number of micronuclei; *t* test; *, $P < 0.05$; **, $P < 0.01$; error bars represent SEM of triplicate datasets. Bars: (A, B, and E) 20 µm; (B and E, insets) 2 µm.

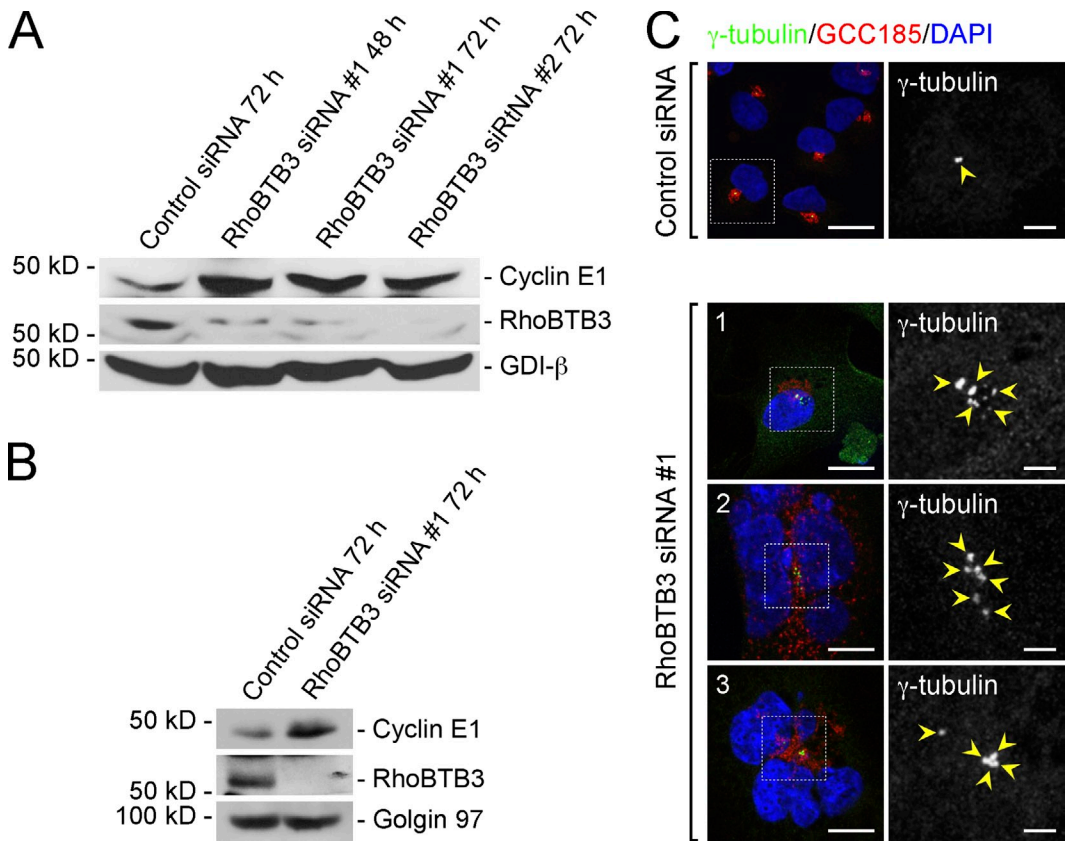

Figure S2. **Increased Cyclin E levels and centrosome overduplication upon RhoBTB3 depletion.** (A) Immunoblot of total HeLa cell lysates shows that Cyclin E1 increases upon depletion of RhoBTB3 with two distinct siRNAs. (B) Immunoblot showing Cyclin E levels in RhoBTB3-depleted U2OS cells. (C) 10% of RhoBTB3-depleted cells (n = 70) show centrosome overduplication (detected with anti–γ-tubulin antibody); three examples are shown. Golgi complexes were identified using anti-GCC185 antibody. Examples 2 and 3 show nuclear atypia and are multinucleated. Bars in merge and inset images are 20 and 5 µm, respectively.

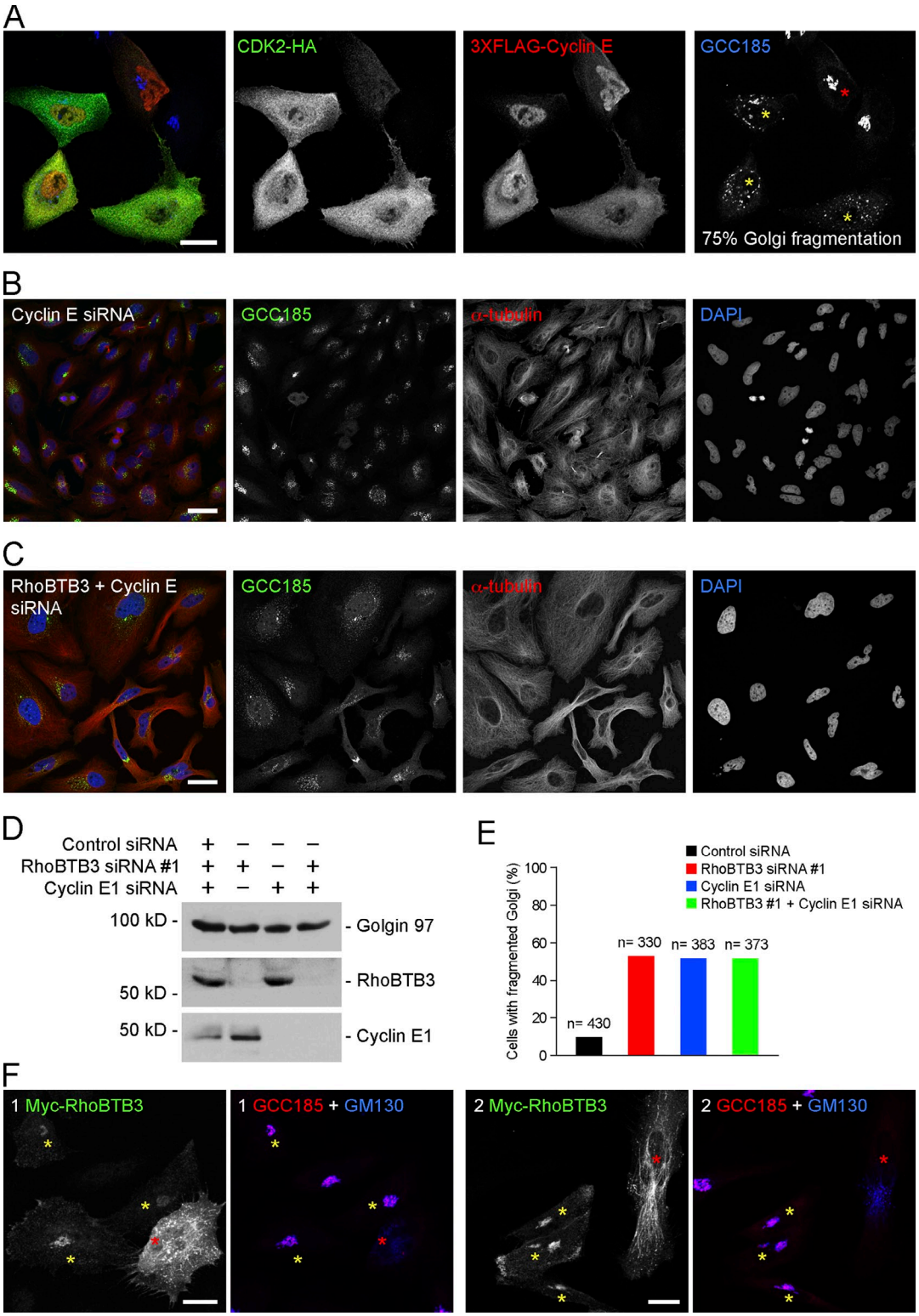

Figure S3. **Involvement of Cyclin E and RhoBTB3 in Golgi structure regulation.** (A) Overexpression of CDK2 with Cyclin E1 causes Golgi fragmentation. Asterisks indicate HeLa cells transfected with both HA-CDK2 and FLAG–Cyclin E1, yielding 75% fragmentation (yellow asterisks); $n = 80$ cells. Golgi complexes of HeLa cells were detected with anti-GCC185. (B–E) Depletion of either Cyclin E1 or RhoBTB3 causes Golgi disruption. HeLa cells were treated with the indicated siRNAs for 72 h and labeled with the indicated antibodies (B and C). (D) Documentation of protein depletion upon siRNA treatment. (E) Quantitation of Golgi fragmentation of Control siRNA (black column), RhoBTB3 siRNA (red column), Cyclin E siRNA (blue column), and RhoBTB3 + Cyclin E siRNA (green column). (F) Myc-RhoBTB3 overexpression disrupts the Golgi. Two fields are shown (1 and 2). Yellow asterisks indicate low expressing, Myc-RhoBTB3-transfected HeLa cells containing "normal" Golgi complexes (detected with anti-GCC185 and anti-GM130 antibodies); red asterisks indicate cells expressing high levels of Myc-RhoBTB3 (see green Myc staining). Bar, 20 μm.

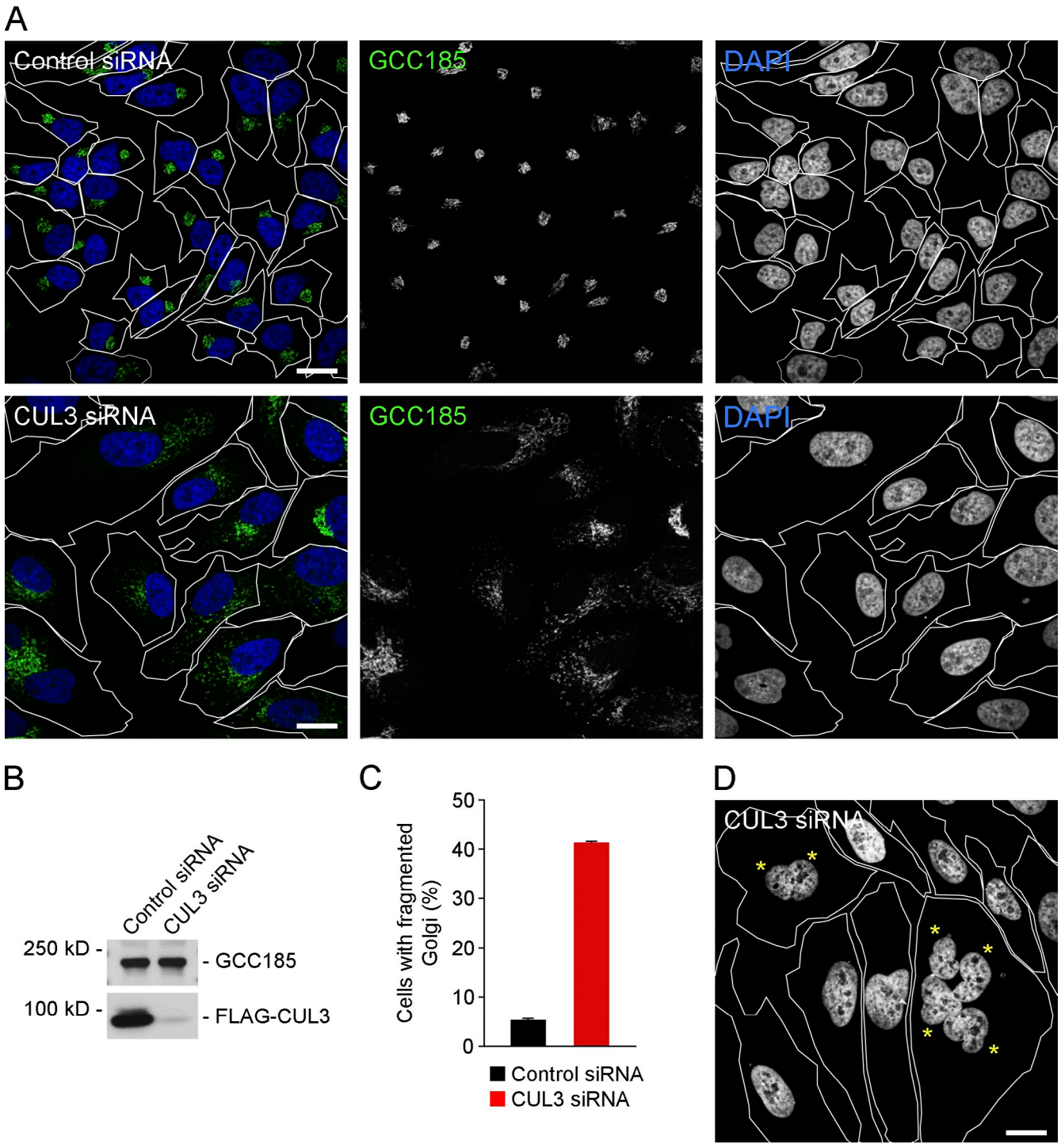

Figure S4. **CUL3 depletion leads to Golgi fragmentation, enlarged cell/nuclear size, and multinuclei formation.** (A) Confocal microscopy of HeLa cells transfected for 72 h with control siRNA or CUL3 siRNAs as indicated and stained for GCC185. DNA was stained with DAPI. (B) Immunoblot detection of CUL3 depletion in HeLa cells. (C) Quantitation of Golgi morphology in control or CUL3-depleted cells. The data represent the mean of two independent data sets in which ≥148 cells were analyzed in both conditions; error bars represent SEM. (D) Presence of multinucleated cells (yellow asterisks indicate nuclei) after 72 h treatment with a CUL3 siRNA. Bar, 20 µm.

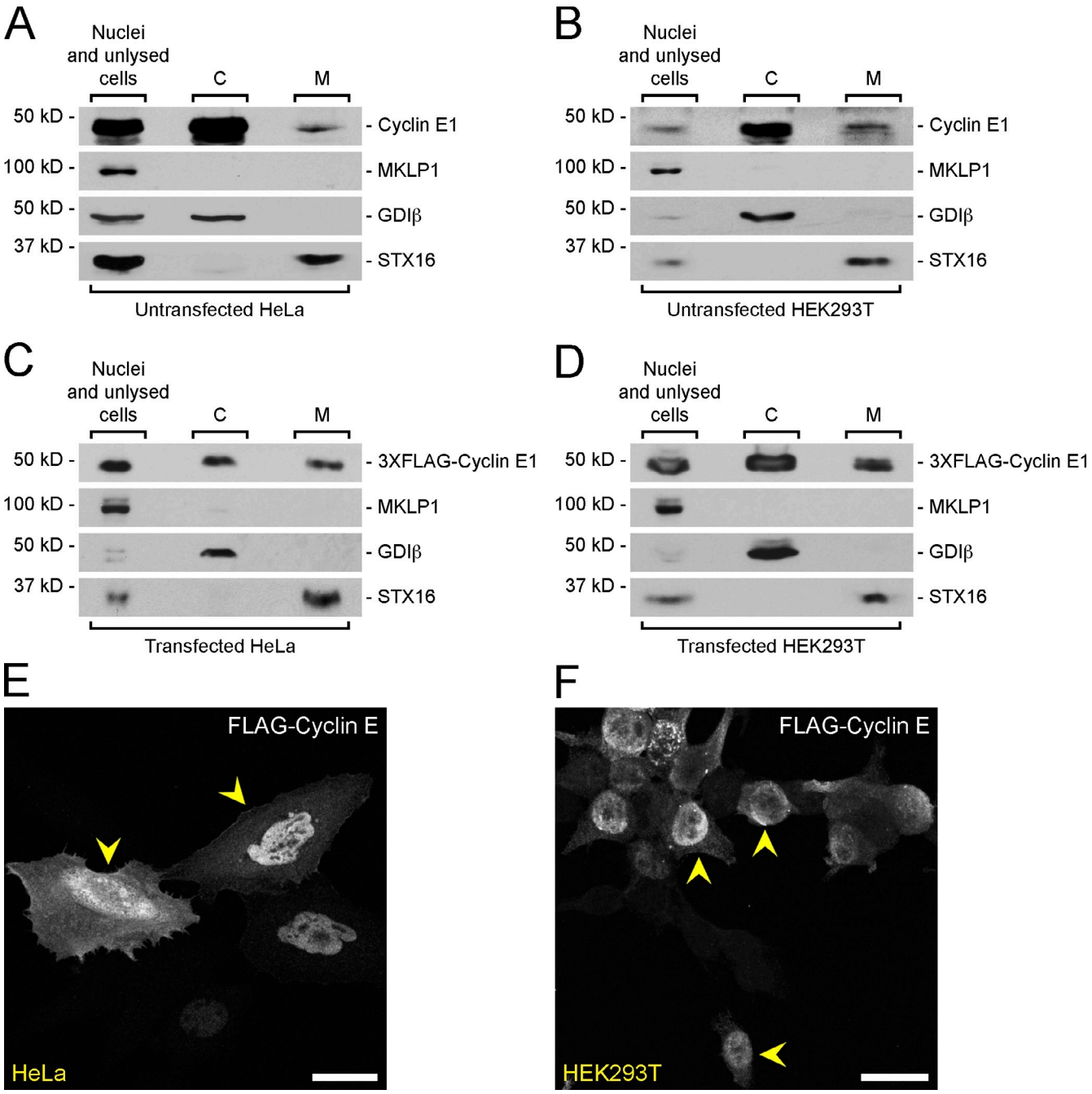

Figure S5. **Subcellular distribution of Cyclin E in human cells.** Subcellular distribution of Cyclin E in HeLa (A and C) or HEK293T cells (B and D), before (A and B) or after (C and D) transfection with Cyclin E1 (A–D). Equal proportions of nuclear, cytosolic (C), or membrane (M) fractions were analyzed. (E and F) Localization of FLAG–Cyclin E in HeLa (E) or HEK293T cells (F) by light microscopy. Arrowheads indicate cells displaying both cytosolic and nuclear pools of protein. Bar, 20 µm.

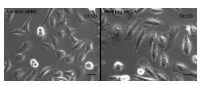

Video 1. **RhoBTB3-depleted cells do not undergo mitosis in vivo.** Time-lapse phase-contrast video microscopy of HeLa cells after 48 h with control (left frames) or RhoBTB3 siRNA #1 (right frames). Cells were imaged every 3.5 min for 15 h using an inverted microscope (Axio Observer Z1; Carl Zeiss) fitted with an LD Plan-Neofluar 20×/0.4 Korr Ph1 Ph2 objective and a CCD camera (AxioCam MRm; Carl Zeiss) controlled by AxioVision 4.8 software (Carl Zeiss). Black arrows in Control siRNA frames indicate cells undergoing mitosis. White arrows at the beginning and at the end of RhoBTB3 siRNA frames show cells that do not enter mitosis and keep growing in size. Bar, 40 µm.